COMPARISON BETWEEN SINGLE AND MULTI-STAGE TRIAXIAL COMPRESSIVE STRENGTHS OF SOME ROCK TYPES

THANAWAT SASEN

A Thesis Submitted in Partial Fulfillment of the Requirements for the Degree of Master of Engineering in Civil, Transportation and Geo-resources Engineering

Suranaree University of Technology

Academic Year 2024

การเปรียบเทียบกำลังกดในสามแกนแบบขั้นตอนเดียวและแบบหลายขั้นตอนของหินบางชนิด

นายธนวัฒน์ ซาเสน

วิทยานิพนธ์นี้เป็นส่วนหนึ่งของการศึกษาตามหลักสูตรปริญญาวิศวกรรมศาสตรมหาบัณฑิต
สาขาวิชาวิศวกรรมโยธา ขนส่ง และทรัพยากรธรณี
มหาวิทยาลัยเทคโนโลยีสุรนารี
ปีการศึกษา 2567

COMPARISON BETWEEN SINGLE AND MULTI-STAGE TRIAXIAL COMPRESSIVE STRENGTHS OF SOME ROCK TYPES

Suranaree University of Technology has approved this thesis submitted in partial fulfillment of the requirements for a Master's Degree.

Thesis Examining Committee

.....

(Assoc. Prof. Dr. Pornkasem Jongpradist)
Chairperson

.....

(Emeritus Prof. Dr. Kittitep Fuenkajorn)
Member (Thesis Advisor)

.....

(Asst. Prof. Dr. Prachya Tepnarong)
Member

.....

(Assoc. Prof. Dr. Yupaporn Ruksakulpiwat)
Vice Rector for Academic Affairs
and Quality Assurance

.....

(Assoc. Prof. Dr. Pornsiri Jongkol)
Dean of Institute of Engineering

ธนวัฒน์ ซาเสน : การเปรียบเทียบกำลังกดในสามแกนแบบขั้นตอนเดียวและแบบหลายขั้นตอนของหินบางชนิด (COMPARISON BETWEEN SINGLE AND MULTI-STAGE TRIAXIAL COMPRESSIVE STRENGTHS OF SOME ROCK TYPES)
อาจารย์ที่ปรึกษา : ศาสตราจารย์ (เกียรติคุณ) ดร.กิตติเทพ เฟื่องขจร, 86 หน้า.

คำสำคัญ: เกณฑ์ Hoek-Brown/ กำลังรับแรงกด/ สัมประสิทธิ์ความยืดหยุ่น/ อัตราส่วนปัวซอง/ วิถีการให้แรง

การศึกษานี้มีจุดประสงค์เพื่อเชื่อมโยงกำลังรับแรงกดแบบสามแกนที่ได้จากการทดสอบแบบหลายขั้นตอนกับการทดสอบแบบขั้นตอนเดียวตามวิธีดั้งเดิม ผลลัพธ์จากหินสิบชนิดถูกใช้เพื่อกำหนดพารามิเตอร์ของ Hoek-Brown ภายใต้แรงดันล้อมรอบตั้งแต่ 0 ถึง 40 เมกะปาสคาล อัตราส่วนของพารามิเตอร์ Hoek-Brown ที่ได้จากการทดสอบแบบหลายขั้นตอนต่อการทดสอบแบบขั้นตอนเดียว (เช่น m_m/m_s) มีความสัมพันธ์ที่ดีกับค่ากำลังรับแรงกดในแกนเดียวของหิน ($R^2 > 0.9$) โดยใช้สมการเลขยกกำลัง ด้วยเหตุนี้ค่ากำลังรับแรงกดแบบสามแกนของหินจึงสามารถคาดการณ์ได้ เมื่อทราบค่าพารามิเตอร์ของ Hoek-Brown ของการทดสอบแบบหลายขั้นตอนและค่ากำลังรับแรงกดในแกนเดียวของหิน อย่างไรก็ตาม ความสัมพันธ์ของค่ากำลังรับแรงระหว่างสภาวะการทดสอบทั้งสองนี้ขึ้นอยู่กับวิถีการให้แรงที่ใช้ระหว่างการทดสอบแบบหลายขั้นตอนเป็นอย่างมาก วิถีการให้แรงที่แตกต่างกันอาจส่งผลให้ความสัมพันธ์ $m_m/m_s - \sigma_c$ แตกต่างกัน พฤติกรรมการเปลี่ยนรูปของหินในระหว่างการทดสอบสามแกนแบบหลายขั้นตอนเน้นการใช้เครื่องกดหินแบบหลายแกนเพื่อวัดการเปลี่ยนรูปทั้งในแนวแกนและแนวด้านข้างแม้ภายหลังจากชิ้นงานเกิดการวิบัติในรอบแรกของการให้แรงแล้ว ผลการศึกษาแสดงให้เห็นว่าอัตราส่วนของปัวซองเพิ่มขึ้นตามแรงดันล้อมรอบระหว่างการทดสอบแบบหลายขั้นตอน ซึ่งแตกต่างกับการลดลงทั่วไปที่สังเกตได้ในการทดสอบแบบขั้นตอนเดียว การศึกษาครั้งนี้ยังพบอีกว่าโมดูลัสความยืดหยุ่น (E_m และ E_s) และโมดูลัสเฉือน (G_m และ G_s) สามารถเชื่อมโยงกันได้โดยใช้สมการที่คล้ายกับสมการของ Goodman (1970) ทำให้สามารถทำนายพารามิเตอร์การเปลี่ยนรูปของหินที่สมบูรณ์จากสภาวะการทดสอบแบบหลายขั้นตอนสำหรับตัวอย่างหินที่เกิดการวิบัติได้

สาขาวิชา <u>เทคโนโลยีธรณี</u>
ปีการศึกษา <u>2567</u>

ลายมือชื่อนักศึกษา .....
ลายมือชื่ออาจารย์ที่ปรึกษา .....

THANAWAT SASEN: COMPARISON BETWEEN SINGLE AND MULTI-STAGE TRIAXIAL COMPRESSIVE STRENGTHS OF SOME ROCK TYPES. THESIS ADVISOR: EMERITUS PROF. DR. KITTITEP FUENKAJORN, Ph.D., P.E., 86 PP.

Keyword: Hoek-Brown criterion, Compressive strength, Elastic Modulus, Poisson's Ratio, Loading path

This study aims at correlating the triaxial compressive strengths obtained from multi-stage testing with those from the conventional single stage test conditions. Results from ten rock types are used to determine Hoek-Brown parameters under confining pressures ranging from 0 to 40 MPa. The ratio of Hoek-Brown parameters obtained from multi-stage testing to that of single stage testing (i.e. m_m/m_s) can correlate well with the rock uniaxial compressive strengths (with $R^2 > 0.9$) using on exponential equation. As a result, the triaxial compressive strength of rock can be closely predicted providing that the Hoek-Brown parameters from multi-stage testing and the uniaxial compressive strengths of the rock are known. The correlation of the strength results between the two test conditions however strongly depends on the loading path used during the multi-stage testing. Different loading paths would likely result in a different $m_m/m_s - \sigma_c$ relation. The deformation behavior of rocks during multi-stage triaxial testing, highlighting the use of a polyaxial load frame to measure both axial and lateral deformations even after specimen failure in the first loading cycle. The results show that Poisson's ratios increase with confining pressures during multi-stage testing, contrasting with the typical decrease observed in single stage testing. The study also finds that the elastic moduli, E_m and E_s, and shear moduli, G_m and G_s can be correlated using equations similar to those by Goodman (1970), allowing predictions of deformation parameters for intact rocks from multi-stage test conditions for failed specimens.

School of Geotechnology
Academic Year 2024

Student's Signature .....
Advisor's Signature .....

ACKNOWLEDGEMENT

I wish to acknowledge the funding support from Suranaree University of Technology (SUT).

I would like to express thanks to Emeritus Prof. Dr. Kittitep Fuenkajorn, thesis advisor, who gave a critical review. I appreciate his encouragement, suggestions, and comments during the research period. I would like to express thanks to Assoc. Prof. Dr. Pornkasem Jongpradist and Asst. Prof. Dr. Prachya Tepnarong for their valuable suggestions and comments on my research works as thesis committee members. Grateful thanks are given to all staffs of Geomechanics Research Unit, Institute of Engineering who supported my work.

Finally, I most gratefully acknowledge my parents for all their support and encouragement throughout the period of this study.

Thanawat Sasen

TABLE OF CONTENTS

Page

TABLE OF CONTENTS (Continued)

Page

TABLE OF CONTENTS (Continued)

Page

LIST OF TABLES

Table **Page**

LIST OF FIGURES

Figure **Page**

LIST OF FIGURES (Continued)

Figure **Page**

LIST OF FIGURES (Continued)

Figure **Page**

SYMBOLS AND ABBREVIATIONS

σ_c	=	Uniaxial compressive strength
σ_1	=	Major principal stress
σ_2	=	Intermediate stress
σ_3	=	Minor principal stress
$\sigma_{1,f}$	=	Major principal stress at failure
ε_1	=	Major principal strains
ε_2	=	Intermediate principal strains
ε_3	=	Minor principal strains
ν_s	=	Poisson's ratio on single stage
ν_m	=	Poisson's ratio on multi-stage
E_s	=	Elastic moduli on single stage
E_m	=	Elastic moduli on multi-stage
G_s	=	Shear modulus on single stage
G_m	=	Shear modulus on multi-stage
m	=	Empirical constant for equation (6.1)
s	=	Empirical constant for equation (6.1)
m_s	=	Empirical constant for equation (6.2 and 6.4)
m_m	=	Empirical constant for equation (6.2 and 6.4)
a	=	Empirical constant for equation (6.2)
b	=	Empirical constant for equation (6.2)
s_s	=	Empirical constant for equation (6.3)
s_m	=	Empirical constant for equation (6.3)
c	=	Empirical constant for equation (6.3)
d	=	Empirical constant for equation (6.3)
β	=	Empirical constant for equation (6.5 and 6.7)
α	=	Empirical constant for equation (6.6 and 6.8)

CHAPTER I
INTRODUCTION

1.1 Background and Rationale

The triaxial compression test (ASTM D7012-14) has been widely used to determine rock strength and deformation under confinement, which are important parameters for the design and stability study of geological structures in civil as well as mining engineering works, including foundations for dams, structures, and bridges, and additional host rocks for underground mining and tunnels. The triaxial compression test is used in the laboratory to simulate these structures. A significant limitation of the traditional triaxial test method is that it is expensive, time-consuming, and requires a large number of standard samples. The multi-stage triaxial compression test (Wang, Feng, Yang, Han, and Kong (2022) and Minaeian, Dewhurst, and Rasouli (2020) and Yang (2012)) is more popular nowadays because it requires fewer samples to determine the triaxial strength. It is found that the multi-stage strength is often lower than the single-stage strength. The differences and representativeness of the multi-stage test results and the deformation modulus however require more investigation.

The multi-stage triaxial test concept was first introduced in the mid-1970s (Kovári and Tisa, 1975). It is necessary to test a variety of rocks to conduct a comparative study of the single-stage and multi-stage strengths. Accurate lateral and axial stresses of the specimen are typically difficult to measure due to non-uniform deformations of the specimen and local strain measurement by measuring equipment (Aghababaei, Behnia, and Moradian, 2019).

1.2 Research Objective

The objective of this study is to develop mathematical correlations between single stage and multi-stage triaxial compressive test results in terms of strength and deformability. Hoek-Brown strength criterion and Goodman stiffness relation between intact and fractured rocks are employed. Ten rock types with strength varying from

soft to strong rocks are used. A polyaxial load frame is used to load and unload the specimens, which allows determining the compressive strengths and deformation moduli of the rocks under both single and multi-stage testing.

1.3 Scope and Limitations

The scope and limitations of the research include as follows:

1) Laboratory testing is conducted on 10 rock types, including Tak Fa gypsum, Maha Sarakham salt, Khao Khad bedded limestone, Phu Kradung sandstone, Khao Khad marble, Pha Wihan sandstone, Phu Phan bedded sandstone, Phu Phan sandstone, Rayoung-Bang Lamung granite, and Buriram basalt.

2) All rectangular rock specimens have nominal dimensions of 54x54x108 mm^3.

3) Polyaxial load frame is employed to apply axial and lateral loads to the specimens.

4) Single and multi-stage triaxial tests use the confining pressures ranges from 0 MPa to 40 MPa.

5) Testing procedures follow the ASTM D7012-14 (2014) standard practice where applicable.

6) All tests are carried out at ambient temperatures.

1.4 Research Methodology

A literature review, sample preparation, laboratory testing (single and multi-stage triaxial compression tests), strength and deformability analysis, mathematical relations, discussions and conclusions, and thesis writing comprise 7 steps during the research methodology depicted in Figure 1.1.

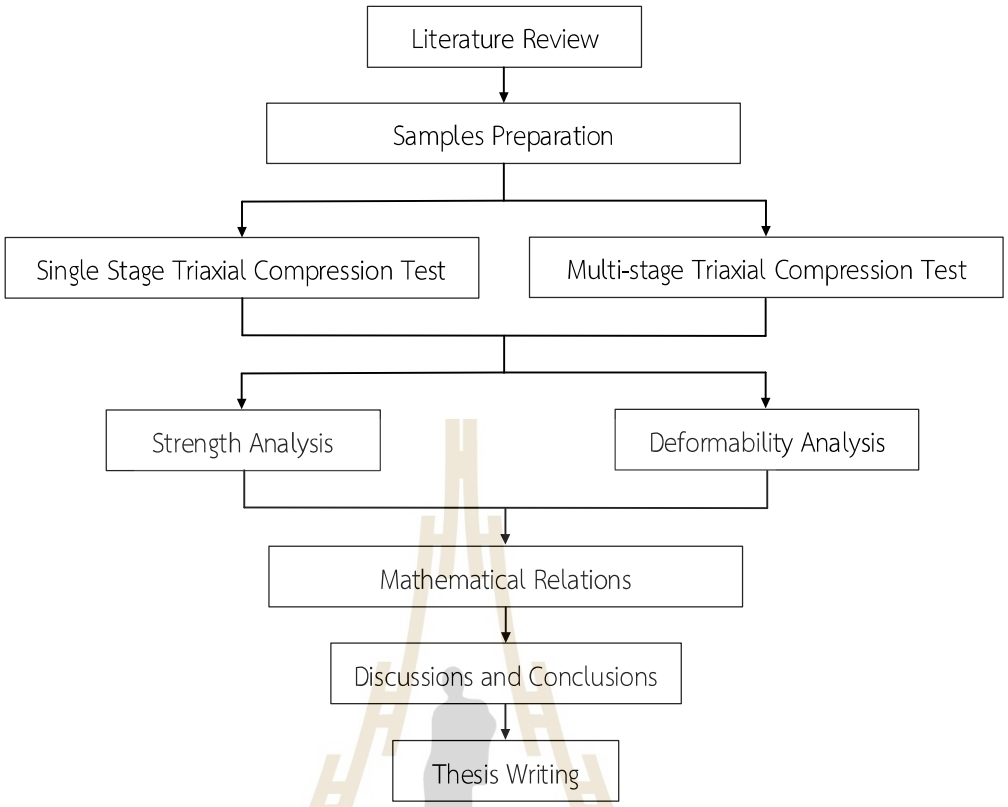

Figure 1.1 Research methodology.

1.4.1 Literature Reviews

Literature review is conducted on experimental studies related to the comparison of single and multi-stage triaxial compressive strengths and deformation moduli. Academic papers, conferences, and journals provide the material for this work. Chapter II offers a synopsis of the literature review.

1.4.2 Samples Collection and Preparation

Rock specimens are prepared from ten different rock types, ranging from soft to hard rock, collected from various locations within Thailand, including Tak Fa gypsum, Maha Sarakham salt, Bedded limestone, Phu Kradung sandstone, Khao Khad marble, Pha Wihan sandstone, Phu Phan bedded sandstone, Phu Phan sandstone, Rayoung-Bang Lamung granite and Buriram basalt. Each specimen is prepared into prismatic specimen with nominal dimension of 54 × 54 × 108 mm^3. For sedimentary rocks, the bedding planes are oriented perpendicular to the major axis to standardize

testing conditions to single stage, while one specimen for multi-stage triaxial compression tests.

1.4.3 Single and multi-stage triaxial compression test

Single and multi-stage triaxial compression tests are conducted using a polyaxial compression frame device (Fuenkajorn, Sriapai, and Samsri, 2012) to directly measure axial and lateral strains during both the loading and reloading phases. These tests are conducted under constant confining pressures ranging from 0 to 40 MPa. To decrease friction, neoprene sheets are positioned at every interaction between the rock surface and the loading plates. The deformation of the sample in axial and lateral orientations is measured using dial displacement gages. This includes the collapsed load, the displacement, and modes of failure. Then, the specimen's strength and elastic parameters are calculated and studied. The multi-stage triaxial strength from just one specimen is used to predict the single stage triaxial strength.

1.4.4 Strength criteria

Hoek-Brown Criteria (Hoek-Brown, 1980), which are used to determine rock mass strength, are applied to the triaxial strength data. They are formulated in the terms of σ_1 and σ_3 at failure. The predictability of these strength is assessed and compared using the coefficient of correlation (R^2). The higher R^2 value shows that the criterion is more predictable and gives consistent values for m and s for correlating the single and multi-stage triaxial compression test results.

1.4.5 Deformation modulus

Empirical relations are employed to estimate the deformation moduli of rock specimens. According to Goodman (1970), the deformation modulus of the single stage triaxial test results is predicted by using the obtained multi-stage triaxial test results.

1.4.6 Mathematical Relations

The mathematical relation developed for the strengths and deformability of the rocks will be applied and compared with the test results obtained elsewhere.

1.4.7 Discussions and Conclusions

Discussions are made to explain the comparison between single- and multi-stage triaxial compressive strengths. Similarities and discrepancies will be identified. Applicability and limitations of the analysis results will be explained. Conclusions are drawn from the experimental and analytical results.

1.4.8 Thesis Writing

All the study activities, methods, and conclusions have been compiled in the thesis.

1.5 Thesis Contents

Chapter I explains the background of issues and the importance of the research. The research objectives, methodology, scope, and limitations are identified. Chapter II provides a summary of the literature review results. Chapter III describes sample preparations. Chapter IV describes the laboratory testing. Chapter V presents the results. Chapter VI describes the testing results analysis. Chapter VII describes the discussion and conclusion of the research results, including recommendations for future research studies.

CHAPTER II
LITERATURE REVIEW

2.1 Introduction

Literature review is conducted on experimental studies that investigate the deformation moduli as well as single and multi-stage triaxial compressive strengths. Data sources include journals, technical reports, and conference proceedings. This chapter presents a summary of the findings from the literature review.

2.2 Single stage vs. Multi–stage triaxial compression test

Prayanto, Nurhandoko, and Sunardi (2022) conduct a study the multi-stage triaxial compression test as a cost-effective alternative to the traditional triaxial compression test. This method is particularly useful for determining the reliability of shear strength parameters in rock or soil samples. The study aimed to obtain key material properties such as Young's modulus, Poisson's ratio, cohesive strength, and the internal friction coefficient, all of which are crucial in geotechnical engineering. Shear strength, a fundamental property of rock and soil, plays a critical role in ensuring the stability of various structures such as foundations, retaining walls, slopes, and embankments. Traditionally, shear strength is determined through laboratory tests conducted on either compacted specimens or samples extracted from exploration drilling. However, variability in soil and rock properties often complicates the assessment process, leading to challenges in accurately characterizing shear strength. To address these issues, the multi-stage triaxial compression test was proposed as an effective method for minimizing the effects of soil variability. This approach allows for the extraction of extensive shear strength data from a single specimen by subjecting it to multiple stages of increasing confining stresses. The results demonstrate that this method is both practical and effective for measuring shear strength, providing comparable outcomes to traditional shear tests. Additionally, the study found significant insights into Poisson's ratio behavior during testing. Specifically, Poisson's ratio was observed to increase as the material approached the yield point. Before reaching the yield point, the ratio was relatively low, peaked at the yield point, and

then decreased after surpassing it. This variation in Poisson's ratio highlights the material's deformation behavior during loading and offers valuable information for geotechnical applications. Overall, the multi-stage triaxial compression test offers a reliable and economical approach for evaluating shear strength and associated parameters, making it a valuable tool for addressing challenges in geotechnical engineering

Aghababaei, Behnia, and Moradian (2019) investigat the effectiveness of single stage triaxial experiments and two variants of the multi-stage triaxial test method: (Crawford and Wylie, 1987) modifies version and the original approach suggested by the International Society for Rock Mechanics (ISRM) (Kovari, Tisa, Einstein, and Franklin, 1983). Their study focused on carbonate rocks subjected to varying confining pressures to evaluate and compare the yield strength results from these methods. The researchers analyze the confidence and prediction intervals for all three testing approaches based on their fit to the yield strength. Multi-stage triaxial tests are useful and economical for determining shear strength values, but specimen integrity must be carefully considered. Crawford and Wylie (1987) modified approach is clearly more dependable option than the ISRM method, especially when maintaining the specimen's structural integrity is essential for accurate results.

Al-Maamori, El Naggar, and Micic (2019) investigate the strength characteristics of swelling Queenston shale, with specimens soaked in various fluids for 100 days. They find that the multi-stage triaxial compression tests were well-suited for studying this type of shale, as it had minimal influence on the measured strength. However, the test's reliability depends on precise monitoring of deformation curves during loading to accurately determine the maximum strength at each confining pressure. Failure to identify the imminent strength at any stage compromises the test's advantage over the traditional single stage triaxial compression tests.

Tsoi and Homenok (2017) conduct multi-stage triaxial compression tests on sandstone specimens, creating Mohr-Coulomb envelopes for each sample. They determine key parameters such as elasticity modulus, Poisson's ratio, elastic limit, and specific energy intensity relative to the loading stage. The results revealed a consistent increase in elastic limit, elasticity modulus, and Poisson's ratio across successive stages, highlighting the variation of these properties under loading-unloading conditions. This

variation should be considered in theoretical stress-strain calculations. However, the study concluded that Mohr-Coulomb envelopes derived from multi-stage tests provide a reliable method for describing sandstone strength, especially in situations with limited core samples. This method serves as an alternative to traditional strength envelope techniques, which rely on separate experimental tests (splitting tensile, uniaxial, and conventional triaxial compression). Furthermore, multi–stage triaxial compression makes it possible to describe the stepwise mechanical behavior of rock from an elastic state to a plastic state.

Yang (2012) investigates stress paths and mechanical behaviors of red sandstone under single-stage and multi-stage triaxial compression tests. The stress path for the single stage triaxial test (Fig. 2.1a) followed the conventional triaxial compression method, while the multi-stage triaxial test (Fig. 2.1b) used a single specimen to evaluate the peak strength under varying confining pressures. This approach allows for efficient confirmation of rock peak strength across different conditions. The study found that the peak strength of red sandstone under multi-stage triaxial compression aligns more closely with the nonlinear Hoek-Brown criterion than the linear Mohr-Coulomb criterion. Additionally, for specimens exhibiting larger post-peak circumferential deformation, the internal friction angle under multi-stage compression was approximately the same as in single stage tests, but the cohesion value was significantly lower. This reduction in cohesion correlates with increased circumferential strain after peak strength, reflecting specimen damage caused by the multi-stage testing process. This damage is interpreted as a loss of cohesion within the sandstone.

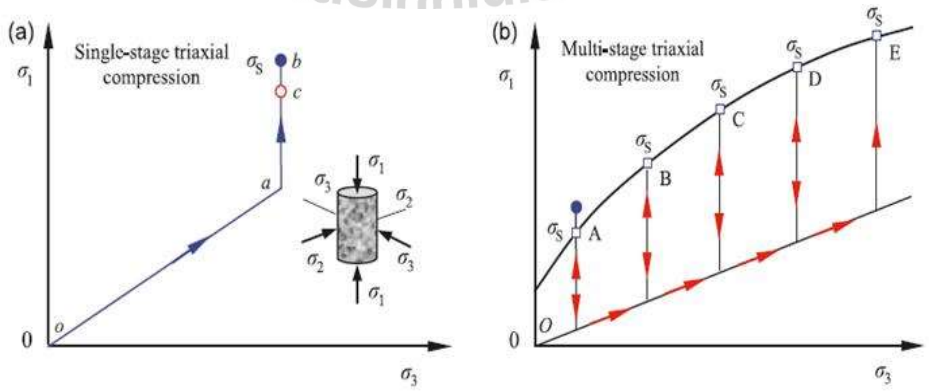

Figure 2.1 Stress path for single stage, (a) and multi-stage triaxial tests (b) (Yang 2012).

Cain, Yuen, Le Bel, Crawford, and Lau (1987) investigate a modified multistage testing procedure provides an accurate determination of the peak strength envelope from a single specimen, with an average discrepancy of approximately +5% compared to single stage tests. This method relies on the volumetric strain/axial strain relationship to predict instability, enabling controlled stage transitions. Unlike the ISRM standard, which maintains the maximum axial stress while increasing confining stress, the modified approach allows partial elastic recovery by relaxing stresses to a hydrostatic level. This adjustment enhances the accuracy of replicating single-stage test conditions. Future improvements, such as servo-controlled confining stress with direct volume change measurement, may further refine the accuracy of this method.

2.3 Factors affecting multi–stage triaxial compression test

2.3.1 Effect of multi–stage triaxial compression test

2.3.1.1 Strength Criteria

Shia et al. (2016) conduct a series of multi-stage triaxial compression tests alongside conventional triaxial tests on sandstone samples to study radial strain variations under different loading paths. The observed variation in radial strain was too minor to effectively compare single and multi-stage tests directly. To address this, they developed a model to correct the strength parameter discrepancies between the two methods. The corrected strength parameters from the multi-stage tests closely matched the conventional triaxial test results, demonstrating the model's effectiveness. Using the Mohr-Coulomb criterion, the data in Figure. 2.2 shows the fitted curve, yielding a high adjusted R-square of 0.932 and an R-square of 0.939, indicating a strong correlation. The fitted parameters included a cohesion value of 22.02 MPa and an internal friction angle of 18.59°, confirming that the Mohr-Coulomb criterion accurately describes the sandstone's strength behaviors.

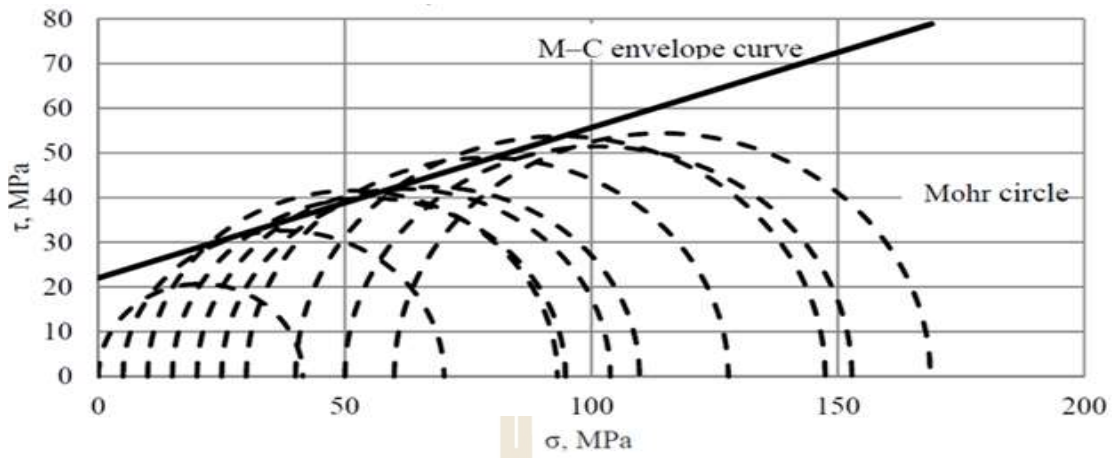

Figure 2.2 Conventional triaxial test data for sandstone (Shia et al., 2016).

Venter, Purvis, and Hamman (2016) conduct a study demonstrates that the intact Hoek–Brown parameters (σ_{ci} and m_i) can be effectively estimated using multistage triaxial testing. This approach optimizes specimen usage, reducing the required number by 80% compared to single-stage testing. Moreover, multistage testing allows for probabilistic analysis due to multiple estimates of σ_{ci} and m_i. However, the study highlights that these parameters are highly sensitive to input variations and should be derived as parameter pairs. Since the research is based on a single homogeneous rock type, further validation across various rock types is necessary.

Yang (2012) investigate the mechanical behavior of red sandstone under multi-stage and single stage triaxial compression, focusing on the relationship between the crack damage threshold and confining pressure (σ_3). The multi-stage triaxial compression findings show that the crack damage threshold increased nonlinearly with higher σ_3 under multi-stage triaxial compression, contrasting with the linear relationship observed in single-stage tests. The difference in crack damage thresholds between the two methods grew as σ_3 increased, indicating that multi-stage loading conditions facilitate easier crack creation and reopening. Importantly, the crack damage threshold in multi-stage triaxial compression was found to be independent of the fractured extent of the specimen's post-peak strength. Single Stage Triaxial Compression Results. The study also presented stress-strain curves for single-stage compression tests (Figure 2.4), showing brittle post-peak behavior even at a high σ_3 of 65 MPa. A transition in failure mode was observed: from class I (stable) at $\sigma_3 = 5$ MPa to class II (unstable) at $\sigma_3 > 5$ MPa. With increasing confining pressure, strain-

softening became more pronounced, while the magnitude of stress drops decreased. This study highlights the distinct differences between multi-stage and single stage triaxial compression tests for red sandstone. Multi-stage loading introduces nonlinear effects on the crack damage threshold and emphasizes the ease of crack initiation and reopening under these conditions. Conversely, single stage tests reveal predictable linear behavior and clear transitions in failure mode and post-peak strain response, providing critical insights into the rock's mechanical behavior.

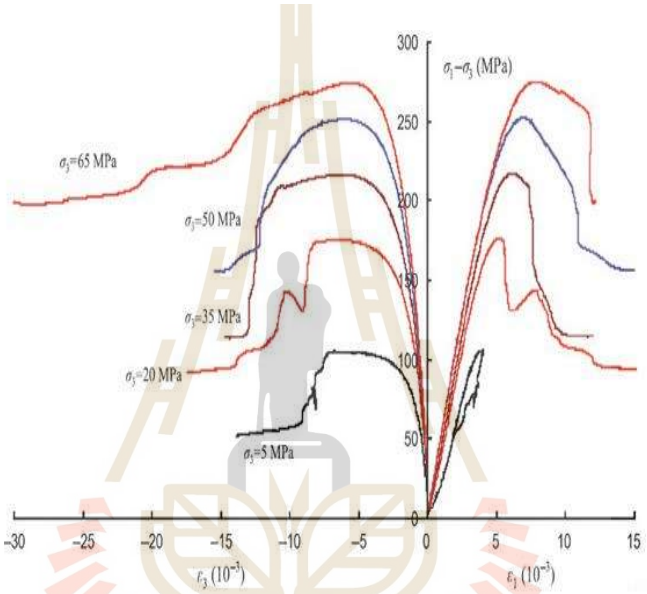

Figure 2.3 Axial deviatoric stress–axial strain and lateral strain curves of red sandstone under triaxial compression test σ_3 = 5 MPa (Yang, 2012).

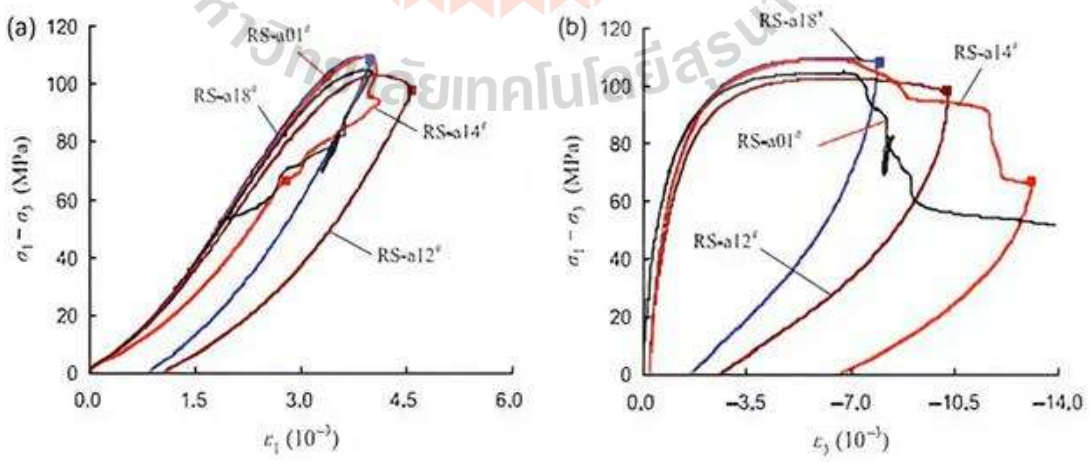

Figure 2.4 Single stage triaxial experimental results of red sandstone. σ_1, axial strain, σ_3, Lateral strain (Yang, 2012).

2.3.1.2 Experimental Techniques

Melati, Wattimena, Kramadibrata, Simangunsong, and Sianturi (2014) investigate how different stress paths impact the results of multi-stage triaxial testing. The study measured stress-strain rates to identify fracture initiation at each stage. The test results were analyzed in terms of the strength envelope and stress-strain curves, as shown in Figure 2.5, and validated using numerical simulations. Multi-stage triaxial tests were conducted on concrete and Tanjung claystone samples using these stress paths. Results showed that both axial load and confining pressure were simultaneously increased. produced higher triaxial compressive strength for both materials. The failure envelopes from this scenario were also closer to those obtained from conventional triaxial tests. Similar findings were noted in studies on Pierre and Raton shale, where constants of failure criteria aligned more closely with single stage triaxial test results. In contrast, tests on Lyons sandstone by (Kim and Ko,1979) yielded different outcomes. This research highlights the significant influence of stress paths on multi-stage triaxial test results, particularly in strength evaluation and failure criteria.

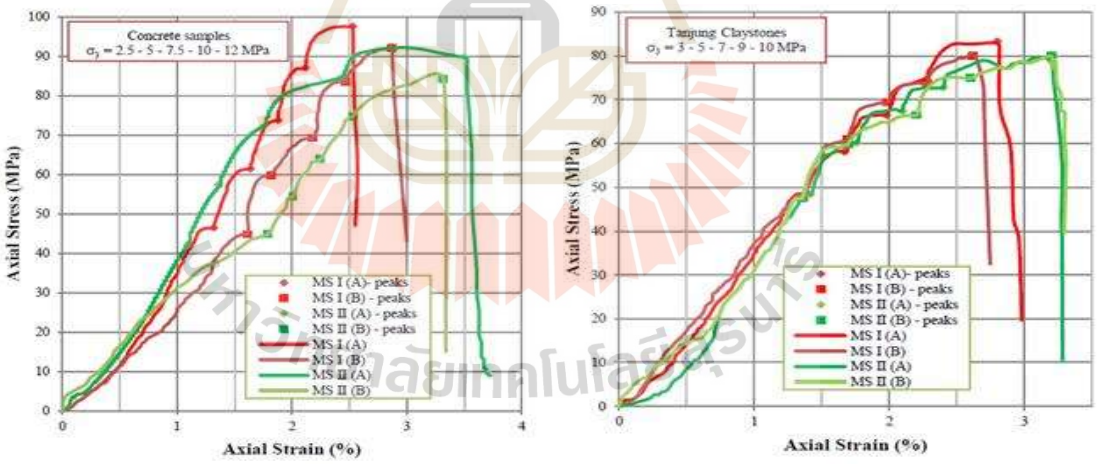

Figure 2.5 Stress-strain curve from multistage triaxial test on: (left) concrete samples, (right) Tanjung claystone (Melati, Wattimena, Kramadibrata, Simangunsong, and Sianturi, 2014).

2.3.1.3 Confining pressure conditions

Hamza, Stace, and Reddish (2005) investigate the impact of strain rate variations on the mechanical properties of silty mudstone, utilizing multi-stage triaxial testing. Experiments were conducted on both intact and fractured rock

samples, revealing that changes in strain rate significantly affect the stiffness and strength of fractured rocks more than intact samples. Slower strain rates caused a notable reduction in the elastic modulus and pre-failure axial stress of fractured samples in Figure. 2.6. The result is attributed to partial creeping and relaxation phenomena. However, at lower confining pressures, these effects were not apparent in intact samples, which diverges from previous findings in other rock types and may be due to the narrow strain rate range used in this study. At higher confining pressures, strain rate impacts on intact samples were minimal, whereas fractured samples exhibited changes under all tested conditions, most notably at 10 MPa confinement. The experimental results were modeled using a non-linear logarithmic function, underscoring the potential sensitivity of medium-to-weak rocks, such as coal measures, to strain rate alterations. The study calls for further exploration into elastic-viscoplastic models and broader strain rate applications to refine understanding and predictive tools across different rock types and conditions.

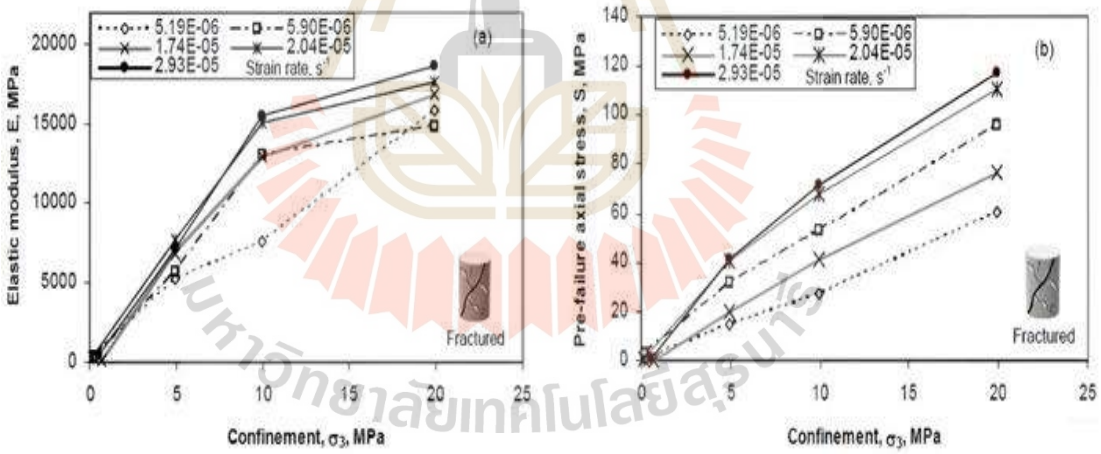

Figure 2.6 Single stage triaxial experimental results of red sandstone. σ_1, axial strain, σ_3, circumferential strain (Hamza, Stace, and Reddish, 2005).

2.3.2 Effect of multi–stage triaxial test on strength and elasticity properties in rock

2.3.2.1 Strength Criteria

Al-Ajmi and Zimmerman (2005) presented the most basic and significant failure criterion in 1776. He proposed that rock failure under compression occurs when the shear stress τ, developed on a particular plane, reaches a value

sufficient to overcome both the natural cohesiveness of the rock and the frictional force opposing motion along the failure plane. The criteria might be expressed as

$$\tau = c + \sigma_n \tan\phi \quad (2.1)$$

where σ_n is the normal stress acting on the failure plane, c is the cohesion of the material, and f is the angle of internal friction. As the sign of t only affects the direction of sliding, Eq. (2.1) should be written in terms of $|\tau|$, but for simplicity we will omit the absolute value sign.

Yang (2012) describes the well-known Mohr-Coulomb and Hoek-Brown criteria as typical strength criteria that have been widely employed in rock mechanics and engineering practice. We study the relationship between multi-stage triaxial strength and the confining pressure using the Mohr–Coulomb and Hoek–Brown criteria. The linear Mohr–Coulomb criterion can be expressed with the following equation:

$$\sigma_s=\sigma_0+q\ \sigma_3=[2C\cos\phi+\sigma_3\cdot(1+\sin\phi)]/(1-\sin\phi) \quad (2.2)$$

where s_0 is usually regarded as the uniaxial compressive strength (UCS) of rock material. The σ_0 and q are related to the cohesion C and the internal friction angle f of rock material.

However, the nonlinear Hoek–Brown criterion is an empirical strength criterion, which can be expressed as the following equation (Hoek and Brown 1980, 1997):

where σ_c is usually regarded as the UCS of intact rock material, m and s are material constants for a specific rock. The parameter s represents the fragmented extent, which

ranges from 0 to 1. The rock remains more complete when the value s approaches 1. By using the linear Mohr–Coulomb Eq. (2.2) and the nonlinear Hoek–Brown Eq. (2.3) criteria, the influence of σ_3 on peak strength σ_s for red sandstone under single-stage and multi-stage triaxial compression is examined. The peak strength values of red sandstone under single and multi-stage triaxial compression can be obtained by these criteria.

2.3.2.2 Deformation modulus

Minaeian, Dewhurst, and Rasouli (2020) investigated the impact of lateral stress anisotropy ($\sigma_2 \neq \sigma_3$) on the mechanical properties and behavior of rock, focusing on compressive strength, elastic modulus, inelastic deformation, dilatancy, and failure modes. They demonstrated that increasing the intermediate principal stress (σ_2) beyond quasi-isotropic conditions ($\sigma_2 = \sigma_3$) led to significant changes in the rock's response. In some cases, the compressive strength more than doubled, and the onset of dilatancy was delayed to over 80% of the peak stress. The measured failure stresses aligned well with the Mogi-type true triaxial failure criterion, indicating that this empirical model effectively captures the rock's behavior under varying stress conditions. To evaluate the effects of σ_2, multi-stage true triaxial tests were performed on synthetic sandstones. In these tests, a single sample was subjected to increasing intermediate principal stress levels while maintaining constant minimum stress. The results were compared with single-stage true triaxial test data, which apply a specific stress configuration to each sample. Distinct differences emerged between the strengths and elastic properties obtained from the two methods, as depicted in Figure 2.7. The study highlighted potential mechanisms underlying these differences, offering insights into the rock's mechanical behavior and supporting the suitability of multistage testing for investigating the influence of intermediate principal stress on rock properties.

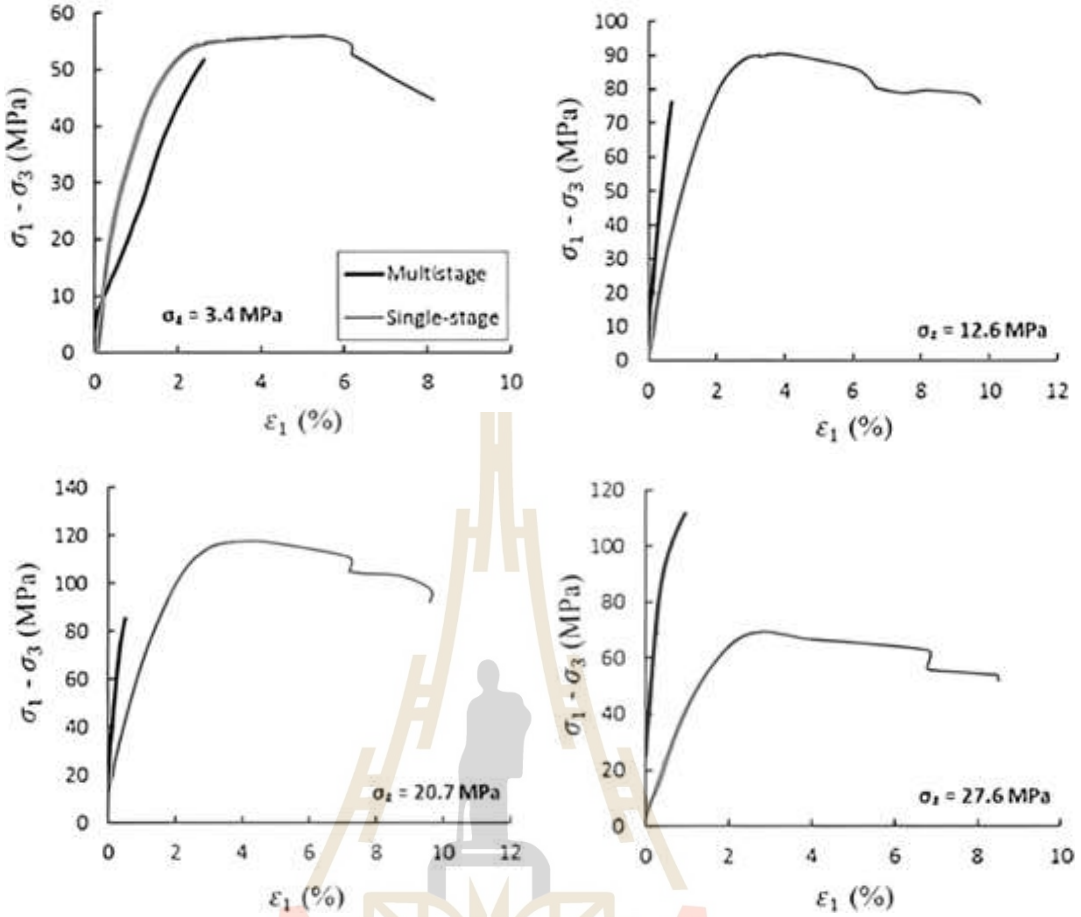

Figure 2.7 Differential stress versus axial strain curves recorded in multi–stage and single stage true triaxial testing of the sandstone samples under σ_3 = 3.4 MPa. (Minaeian, Dewhurst, and Rasouli, 2020).

Yang, Ni, and Wen (2014) examine the spatial evolution of acoustic emission (AE) distribution in red sandstone during multi-stage triaxial deformation under five different confining pressures. This analysis sheds light on the re-fracture deformation mechanisms in pre-damaged specimens. Their findings revealed that both the peak strength and crack damage threshold of red sandstone under multi-stage triaxial compression increase nonlinearly with higher confining pressures (σ_3), as illustrated in Figure 2.8. Furthermore, the disparity between peak strength and crack damage threshold widens as σ_3 increases. These results emphasize the significant influence of confining pressure on the progressive failure characteristics of red sandstone, providing valuable insights into the mechanical behavior of pre-damaged rocks under varying stress conditions.

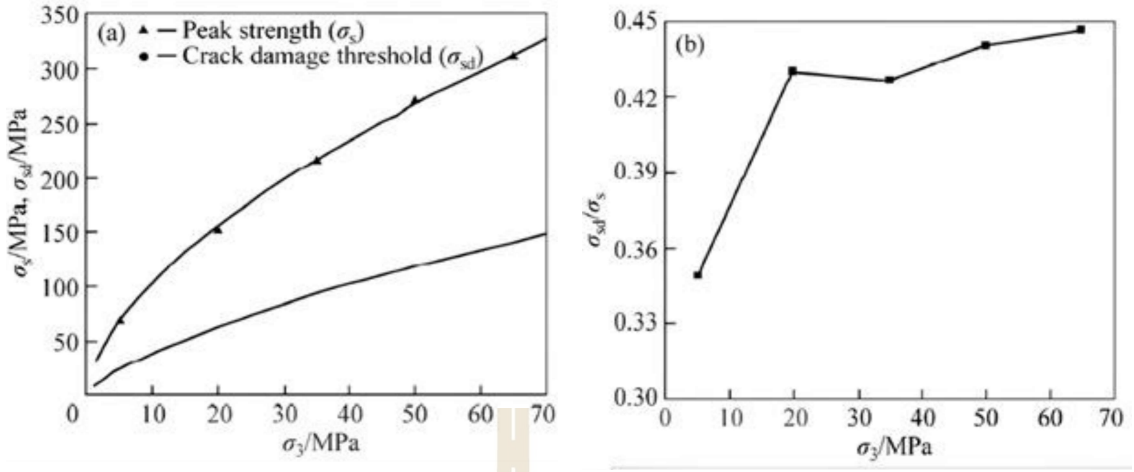

Figure 2.8 Relationship between peak strength, crack damage threshold of red sandstone under multi-stage triaxial compression and confining pressure: (a) σ_s and σ_{sd}; (b) σ_{sd} / σ_s (Yang, Ni, and Wen, 2014).

Yang (2012) states that confining pressure has a significant effect on the deformation parameters of red sandstone under multi-stage triaxial compression, which are lower than those under single stage triaxial compression (Youn and Tonon, 2010). Under both single and multi-stage triaxial compression, the elastic modulus of red sandstone increases with confining pressure, but its increasing values differ depending on the cracked extent of the specimen following peak strength. The elastic modulus is more sensitive to the confining pressure for the specimen with more compressed post-peak circumferential deformation. Red sandstone during multi-stage triaxial compression has a Poisson's ratio larger than that under single stage triaxial compression. Red sandstone's peak axial strain grows nonlinearly under multi-stage triaxial compression; its peak circumferential strain has no known connection with the confining pressure.

Goodman (1970) has introduced a method for assessing the elastic constants of an equivalent continuous material that is representative of a rock mass and is frequently traversed by a single set of joints. This method is based on the concept of joint stiffness. The criterion can be written as:

$$\frac{1}{E_r} = \frac{1}{k_n s} + \frac{1}{E_i} \tag{2.4}$$

where E_r is the rock deformation modulus, k_n is the joint normal stiffness, s is the average joint spacing and E_i is the equivalent deformation modulus.

Thaweeboon, Dasri, Sartkaew, and Fuenkajorn (2016) modified Goodman's (1970) equation to calculate the deformation modulus along three principal directions. The parameter N is proposed whose value depends on joint set direction. The proposed equation can only predict the deformation modulus in the directions normal and parallel to the joint planes. It is proposed as:

$$\frac{1}{E_m} = \frac{N}{k_n s} + \frac{1}{E_i} \tag{2.5}$$

where E_m is the jointed rock deformation modulus, E_i is the intact deformation modulus, s is the joint spacing, k_n is the joint normal stiffness, and N is a parameter whose value varies with the joint set direction (Table 2.1).

Table 2.1 Parameter N defined for modified Goodman's equation.

Number of joint sets	Orientation of joint set to σ_1	Case	N
1	1 parallel		0.5*
1	1 normal		1.0* (original Goodman)
2	1 parallel, 1 normal	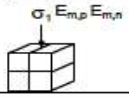	1.5
3	2 parallels, 1normal	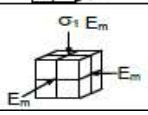	2.0*

2.4 Mechanical Behaviour of rock Under single and multi–stage triaxial compression test.

Wang, Feng, Yang, Han, and Kong (2021) investigate the reliability of rapid procedures employed to determine the mechanical parameters of Jinping marble through true triaxial multistage loading experiments. This work investigated the multistage loading strength, deformation features, and failure mode of the marble based on the findings of three types of multistage loading tests conducted on Jinping marble. Test data lead one to the following conclusions. The Jinping marble true triaxial multistage loading test has been validated. The strength obtained from the multi-stage loading test is somewhat lower than that obtained from the single-stage loading test due to unloading under a fixed condition before the peak strength; yet the difference between the two strength parameters obtained by the Mogi–Coulomb criterion (Al-Ajmi and Zimmerman, 2005) fitting is rather small in Figure 2.9. In engineering, these variations are usually minor. Marble with clearly plastic portions would be suited for the real triaxial multi-stage loading test. To minimize the effect of microfracturing on the strength values, the unloading point should not surpass the peak strength of the specimen during the test. By means of the last stage of the multi-stage loading test, someone can assess the potential error of the strength parameters to confirm the dependability of the chosen data set. For reference in engineering practice, the Jinping marble multi-stage loading test shows good reproducibility and can quickly acquire dependable strength criteria. The macro-mechanical characteristics of Jinping marble under various multi-stage loading situations are shown by the test results to be closely correlated with the formation of interior microcracks. By means of the failure mode analysis, we find that internal microcrack development influences the macro failure mode of the specimen under real triaxial multi–stage stress.

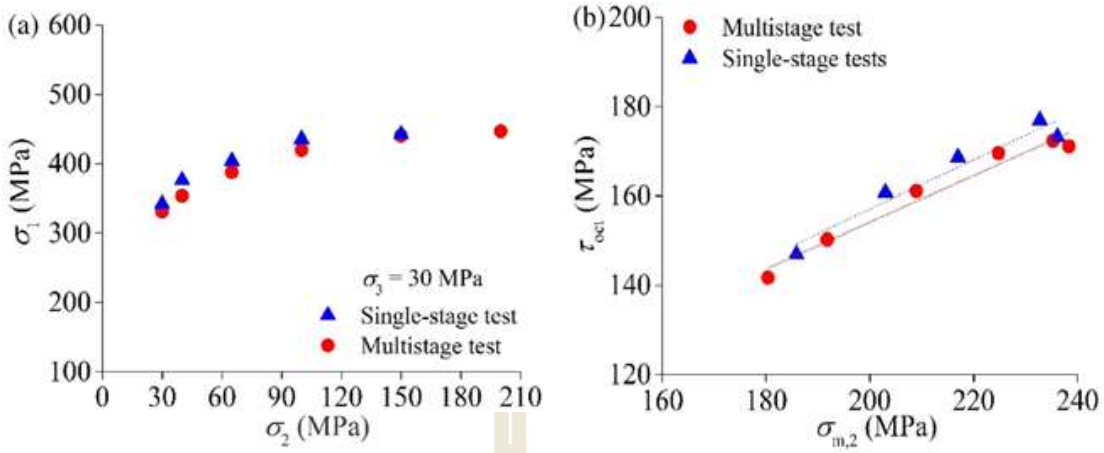

Figure 2.9 Comparative analysis of single and multi-stage tests (a) comparison of strength (b) Mogi–Coulomb strength data fitting comparison. (Wang, Feng, Yang, Han, and Kong, 2021).

Yang et al. (2019) investigate the strength reduction and damage mechanical behavior of mudstone from the Yuncheng coal mine in Shandong province, China, at a depth of 960 m. Using both experimental testing and numerical simulation methods, they examined the mechanical behavior of mudstone under conventional and multi-stage triaxial compression and analyzed their findings, leading to the following conclusions:

1. The Particle Flow Code (PFC) proved effective in simulating the mechanical behavior of mudstone under both conventional and multi-stage triaxial compression at various confining pressures.

2. The peak strength of intact and damaged mudstone specimens increased with confining pressure and adhered well to the linear Mohr–Coulomb criterion. However, the cohesion and internal friction angle of intact specimens were consistently higher than those of damaged specimens, and these strength parameters attenuated with increasing damage extent. The study derived exponential attenuation equations linking cohesion and internal friction angle to the post-stress reduction ratio, with good agreement between experimental and numerical results.

3. A damage variable was defined as the ratio of the micro-crack area to the total specimen area. With increasing post-stress reduction ratio, the damage variable

rose rapidly before stabilizing at a constant level when the ratio exceeded 0.4. Additionally, under reducing confining pressure, the rate of micro-crack formation increased more significantly than under single stage triaxial compression, reflecting a heightened sensitivity of the damaged specimens to stress variations.

These studies highlight the dynamic mechanical behavior and damage mechanisms of mudstone under stress conditions, providing valuable insights for understanding the strength reduction in geological materials subjected to multi-stage deformation.

Vergara, Kudella, and Triantafyllidis (2015) explore the mechanical behavior of bedded and jointed rock to inform the design of slopes, tunnels, and tunnel portals for a planned rail line. Triaxial tests conducted on the material demonstrated ductile behavior, supporting the use of the multi-stage testing technique to evaluate mechanical properties. The study revealed that strength parameters derived from the multi-stage tests were influenced by material composition, failure mode, and confining stress. The observed failure modes highlighted the role of material composition and the presence of discontinuities in determining the failure behavior and resulting strength of the rock specimens. Based on the Mohr–Coulomb failure criterion, the internal friction angle obtained from tests with decreasing confining stress was found to approximate that of intact rock, whereas tests with increasing confining stress showed a contrasting trend. For cohesion, the opposite pattern was observed, with decreasing confining stress tests producing results more divergent from the intact material values. These studies underscore the importance of considering material heterogeneity and discontinuities when assessing the strength and deformation characteristics of bedded and jointed rock for engineering applications.

Amann, Kaiser, and Button (2012) investigate the brittle failure behavior of clay shale under triaxial compression, revealing key insights into its fracture mechanisms. The study found that brittle failure is consistently initiated at a differential stress of 2.1 MPa, indicating negligible friction mobilization at the onset of failure. Volumetric behavior prior to rupture was found to depend on confining stress, as shown in Figures 2.10 and 2.11. At low confining pressures ($\sigma_3 < 0.5$ MPa), volumetric strain at rupture was negative (indicating expansion). As confinement increased, dilation was increasingly suppressed, and for $\sigma_3 \geq 2$ MPa, volumetric strain reversal disappeared entirely,

reflecting the suppression of dilatant fracturing and an associated shift in the failure mode. The rupture surface's characteristics also varied with confining stress. At low confinement ($\sigma_3 < 0.5$), failure planes were steeply inclined, consisting of axial cracks interconnected with bedding-parallel shears. As confinement increased, axial cracks became shorter while bedding-parallel shears extended, and eventually, inclined fractures predominated with axial fractures no longer visible. These observations indicate a transition from axial splitting to macroscopic shear failure as confinement increases. Although crack initiation occurred at a consistent differential stress, rupture stress depended on confining pressure, suggesting the mobilization of friction during failure. The study noted that neither the linear Mohr–Coulomb criterion nor the non-linear Hoek–Brown failure envelope adequately captured the stress dependence of failure. Instead, the data supported a bi- (or tri-) linear or S-shaped failure envelope (e.g., Kaiser and Kim, 2008) to account for the evolving fracture processes. This research highlights the importance of understanding stress-dependent fracture mechanisms in brittle materials like clay shale and offers refined models for capturing complex failure behaviors under varying confining pressures.

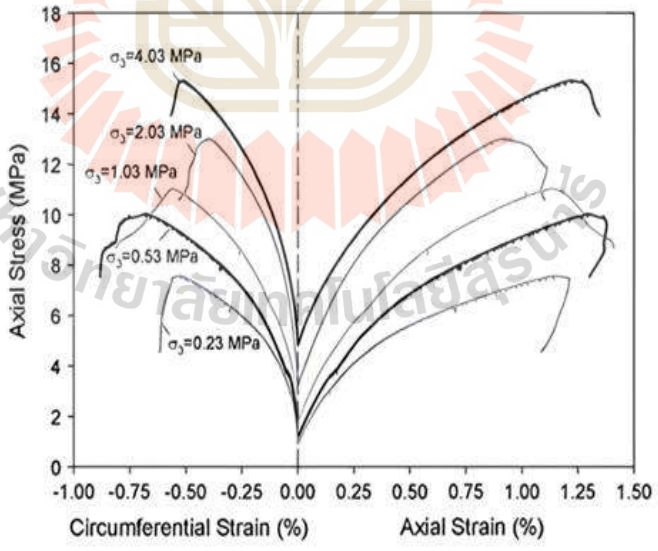

Figure 2.10 Axial and radial strain behavior at different confining stress levels (Amann, Kaiser, and Button, 2012)

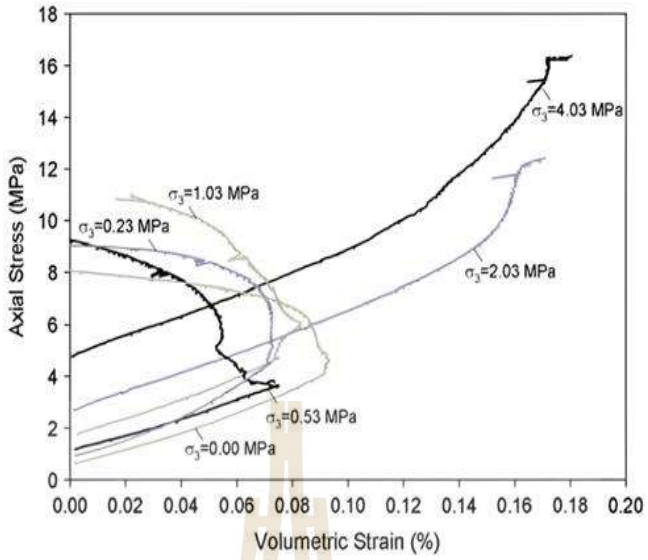

Figure 2. 11 Volumetric strain versus axial stress behavior for different confining stresses in the pre-rupture phase. For confining stress $\sigma_3 \geq \sigma_2$ MPa. (Amann et al., 2012)

CHAPTER III
SAMPLE PREPARATION

3.1 Introduction

This chapter describes rock samples used in this study collected from diverse areas of Thailand (Figure 3.1) to evaluate the single and multi-stage testing conditions. Types and names of the rocks are provided. Specimen dimensions follow the ASTM D7012-14 (2014) standard practice.

3.2 Rock Types and Names

Rock specimens come from various locations in Thailand. Table 3.1 shows the rock data, including period, rock unit, rock code, and rock types. The rock codes provided in the table correspond to those published by DMR (2007, 2010, and 2011). Rock specimens are prepared from ten different rock types, ranging from soft to hard rocks, including Tak Fa gypsum, Maha Sarakham salt, Khao Khad bedded limestone, Phu Kradung sandstone, Khao Khad marble, Pha Wihan sandstone, Phu Phan bedded sandstone, Phu Phan sandstone, Rayoung-Bang Lamung granite, and Buriram basalt.

3.3 Rock sample preparation

Prismatic specimens are prepared with nominal dimensions of 54 × 54 × 108 mm^3. The bedding planes for sedimentary rocks are oriented perpendicular to the primary axis (Figure 3.2). Tables 3.2 and 3.3 show single and multi-stage triaxial test specimen dimensions and density

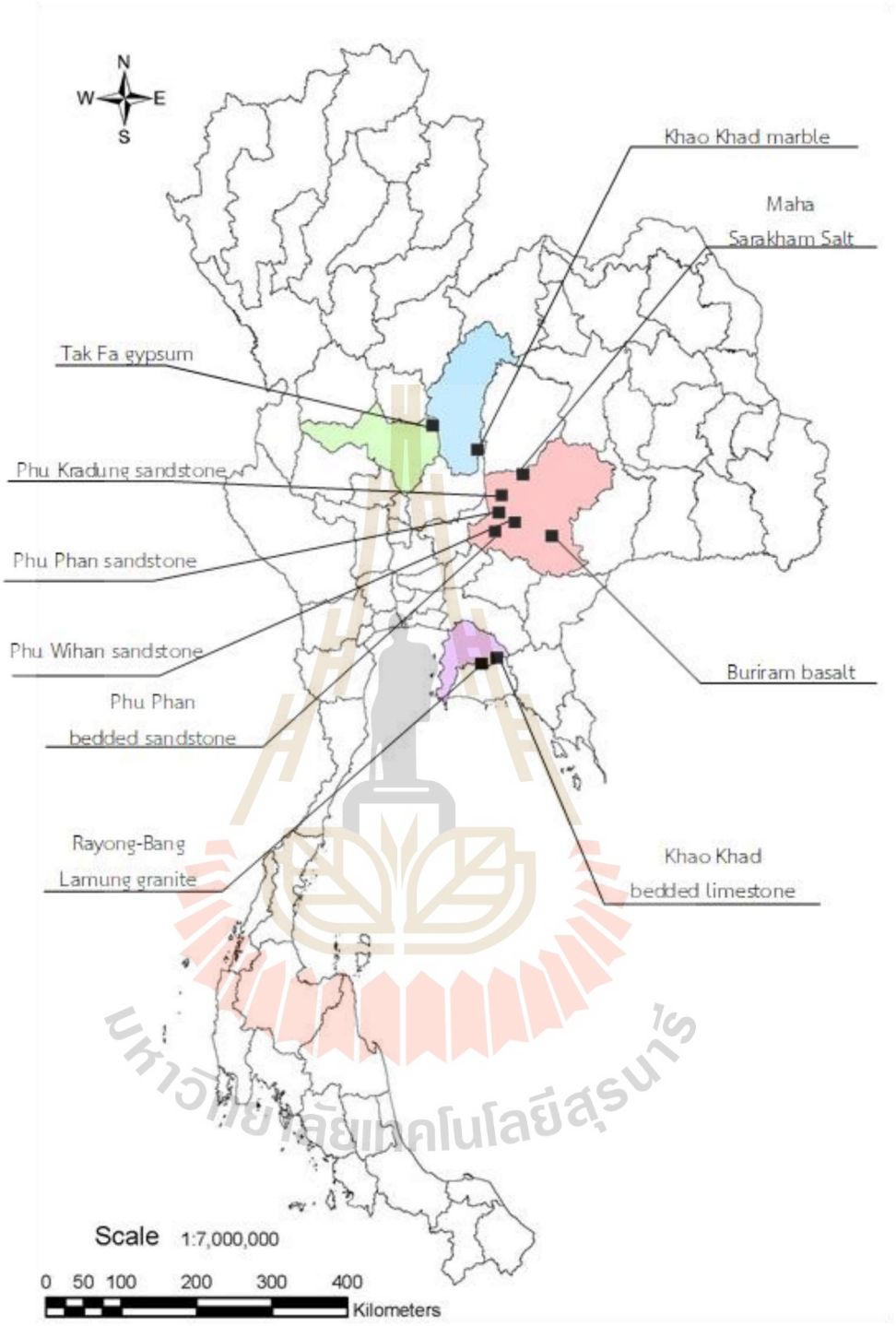

Figure 3.1 Locations at which rock specimens are collected for this study

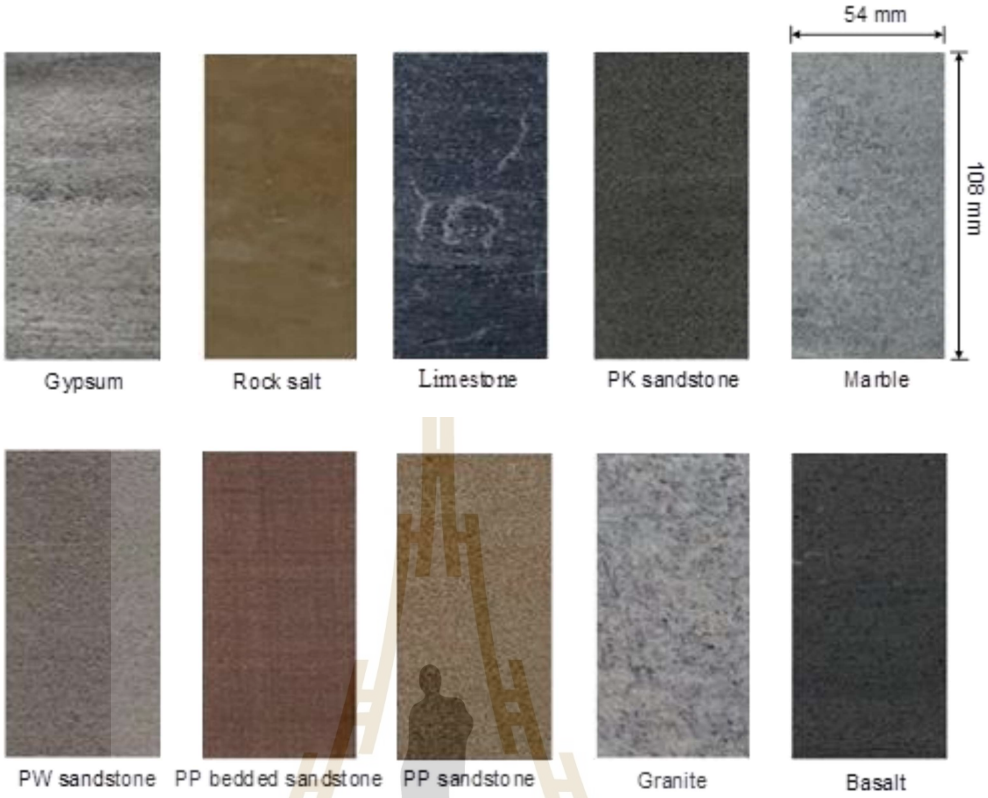

Figure 3.2 Some specimens prepared for single and multi-stage triaxial compression tests

Table 3.1 Rock units and locations from which they are obtained.

Type of rocks	Period*	Code	Locations	Sources
Tak Fa Gypsum	P - C	Tkb	Nakhon Sawan	DMR (2007)
Maha Sarakham Salt	K	KTms	Nakhon Ratchasima	DMR (2010)
Khao Khad bedded limestone	TR - P	PR	Chonburi	DMR (2011)
Phu Kradung sandstone	K	Jpk	Nakhon Ratchasima	DMR (2010)
Khao Khad marble	P	Pkd	Lopburi	DMR (2007)
Pha Wihan sandstone	J	JKpw	Nakhon Ratchasima	DMR (2010)
Phu Phan bedded Sandstone	K-J	Kpp	Nakhon Ratchasima	DMR (2010)
Phu Phan Sandstone	K-J	Kpp	Nakhon Ratchasima	DMR (2010)
Rayong-Bang Lamung granite	T	Rgr	Chonburi	DMR (2011)
Buriram basalt	T	bs	Nakhon Ratchasima	DMR (2010)

* Carboniferous (C), Permain (P), Tertiary (T), Triassic (TR), Jurassic (J), and Cretaceous (K)

Table 3.2 Dimensions and densities of specimens prepared for uniaxial and triaxial compression testing.

Type of rocks	Specimen No.	Width (mm.)		Length (mm)	Weight (g)	Density (g/cc)
		Parallel to Strike	Normal to Strike			
Tak Fa Gypsum	GS-UCS-01	54.2	54.0	107.32	685.43	2.18
	GS-TRI-02	54.1	54.0	107.38	695.32	2.22
	GS-TRI-03	53.7	54.5	106.74	687.36	2.20
	GS-TRI-04	54.1	53.9	106.36	689.31	2.22
	GS-TRI-05	54.5	54.6	106.98	702.31	2.21
Maha Sarakham Salt	S-UCS-01	54.0	54.0	107.70	661.32	2.11
	S-TRI-02	54.1	54.1	108.52	678.32	2.13
	S-TRI-03	53.9	54.4	108.84	675.31	2.12
	S-TRI-04	54.7	53.7	108.92	679.65	2.12
	S-TRI-05	53.6	53.8	106.32	661.31	2.15
Khao Khad bedded limestone	LS-UCS-01	54.0	54.0	108.98	832.15	2.62
	LS-TRI-02	54.7	53.9	109.02	846.52	2.63
	LS-TRI-03	54.7	53.6	107.36	843.16	2.68
	LS-TRI-04	53.8	54.4	106.52	825.47	2.65
	LS-TRI-05	54.7	54.1	107.84	851.24	2.67
	LS-TRI-06	54.1	53.7	107.32	821.74	2.64
Phu Kradung sandstone	PK-UCS-01	54.4	53.0	106.52	708.25	2.30
	PK-TRI-02	54.8	54.4	107.62	742.11	2.31
	PK-TRI-03	54.3	54.8	107.88	738.65	2.30
	PK-TRI-04	53.7	55.0	108.38	754.32	2.36
	PK-TRI-05	53.1	53.9	106.26	719.84	2.37

Table 3.2 Dimensions and densities of specimens prepared for uniaxial and triaxial compression testing. (cont.)

Type of rocks	Specimen No.	Width (mm.)		Length (mm)	Weight (g)	Density (g/cc)
		Parallel to Strike	Normal to Strike			
Khao Khad marble	MR-UCS-01	54.9	54.0	106.62	828.98	2.62
	MR-TRI-02	53.7	53.4	107.02	819.33	2.67
	MR-TRI-03	53.3	54.0	106.32	815.36	2.66
	MR-TRI-04	54.1	54.1	108.52	824.77	2.60
	MR-TRI-05	53.7	53.3	107.30	805.32	2.63
	MR-TRI-06	54.4	53.7	106.86	812.55	2.60
Pha Wihan sandstone	PW-UCS-01	54.0	53.9	106.74	732.15	2.36
	PW-TRI-02	54.2	54.1	106.36	741.11	2.38
	PW-TRI-03	53.4	53.6	106.98	719.19	2.35
	PW-TRI-04	53.9	54.0	106.52	716.55	2.31
	PW-TRI-05	54.2	54.4	107.62	729.32	2.30
	PW-TRI-06	54.4	53.6	107.88	731.31	2.33
	PW-TRI-07	53.4	53.7	108.38	738.95	2.38
Phu Phan bedded Sandstone	PPBSS-UCS-01	54.4	54.3	107.02	721.35	2.28
	PPBSS-TRI-02	53.4	54.1	106.32	732.15	2.39
	PPBSS-TRI-03	54.4	53.4	108.52	729.85	2.32
	PPBSS-TRI-04	53.7	53.0	107.88	721.54	2.35
	PPBSS-TRI-05	54.9	54.4	108.38	749.32	2.32
Phu Phan Sandstone	PPSS-UCS-01	54.3	54.0	106.26	721.36	2.31
	PPSS-TRI-02	54.0	54.2	106.62	731.54	2.34
	PPSS-TRI-03	53.1	53.0	107.36	718.36	2.38
	PPSS-TRI-04	54.3	53.9	106.52	732.55	2.35
	PPSS-TRI-05	54.1	54.4	107.84	729.87	2.30

Table 3.2 Dimensions and densities of specimens prepared for uniaxial and triaxial compression testing. (cont.)

Type of rocks	Specimen No.	Width (mm.)		Length (mm)	Weight (g)	Density (g/cc)
		Parallel to Strike	Normal to Strike			
Rayong-Bang Lamung granite	GR-UCS-01	53.7	54.7	108.52	812.36	2.55
	GR-TRI-02	54.8	53.3	107.88	817.77	2.59
	GR-TRI-03	55.0	54.0	108.38	805.36	2.50
	GR-TRI-04	53.3	55.0	106.32	799.25	2.57
Buriram basalt	BS-UCS-01	53.9	53.3	107.36	836.52	2.71
	BS-TRI-02	54.0	53.8	106.52	856.32	2.76
	BS-TRI-03	54.1	54.5	107.84	865.36	2.72
	BS-TRI-04	53.7	54.7	108.52	887.77	2.79
	BS-TRI-05	53.8	54.1	107.88	871.36	2.77

Table 3.3 Dimensions and densities of specimens prepared for multi-stage triaxial compression testing.

Type of rocks	Specimen No.	Width (mm.)		Length (mm)	Weight (g)	Density (g/cc)
		Parallel to Strike	Normal to Strike			
Tak Fa Gypsum	GS-MST-01	54.0	54.0	107.68	695.3	2.21
Maha Sarakham Salt	S-MST-01	54.3	53.5	108.32	672.3	2.13
Khao Khad bedded limestone	LS-MST-01	53.9	54.0	109.02	825.4	2.60
Phu Kradung sandstone	PK-MST-01	54.3	54.0	108.46	732.5	2.30
Khao Khad marble	MB-MST-01	53.9	54.4	107.32	819.3	2.61
Pha Wihan sandstone	PW-MST-01	54.0	54.3	108.34	732.7	2.31
Phu Phan bedded Sandstone	PPBSS-MST-01	54.3	53.0	109.22	742.3	2.36
Phu Phan Sandstone	PPSS-MST-01	54.1	54.9	110.02	765.3	2.34
Rayong-Bang Lamung granite	GR-MST-01	53.2	53.2	108.32	785.3	2.56
Buriram basalt	BS-MST-01	54.7	53.8	107.64	865.3	2.73

CHAPTER IV
TEST METHOD AND APPARATUS

4.1 Introduction

This chapter describes laboratory testing methods and apparatus. This applies to triaxial stress conditions. There are two types of triaxial tests: single stage triaxial compression tests and multi-stage triaxial compression tests. The effects of confining pressure on the rock deformations and compressive strengths have been investigated. The results are compared with the results from other studies performed elsewhere.

4.2 Single stage triaxial compression test

The objective of the triaxial compression tests is to determine the parameters (m and s) of the specimens in accordance with the Hoek-Brown criterion (Hoek-Brown, 1980) under varying confining pressures. After the confining pressure is increased a desired magnitude, the axial stress increases at rate of 1 MPa/s until failure occurs while the confining pressure is maintained constant. To find the strength envelope, the specimens are tested at different confining pressures in a single-stage behavior under axial stress until it fails, as per the ASTM standard procedure (ASTM D7012-14). The polyaxial load frame device (Fuenkajorn, Sriapai, and Samsri, 2012) applies axial and lateral loads to the specimens. Two pairs of cantilever beams, each measuring 152 cm in length, apply the lateral stresses in directions that are perpendicular to one another. The outside end of each beam is pulled downward by dead weights on a lower steel bar that connects the two opposing beams underneath. The inner end of the beam is hinged by a pin that is positioned between vertical bars on either side of the frame. As seen in Figure 4.1, all of the beams are positioned almost horizontally during testing, which places a lateral compressive force on the specimen at the center of the frame. Fuenkajorn et al. (2012) conducted a thorough analysis of the polyaxial load frame. Following the rectangular specimen's installation into the load frame, dead weights are positioned on the steel bar to determine the specimen's uniform lateral stress (σ_3), which has been predetermined. A 100-ton hydraulic jack is used to increase the vertical stress at the predetermined pace to begin the test. Throughout the testing, a dial gage

accurately recorded the axial and lateral strains. The specimens' surface friction will be decreased by placing neoprene sheets between all interfaces and loading plates, and the failure stresses are then noted (Fig. 4.2). The results are plotted in the forms of axial stress-strain relations. Both axial and lateral deformations are recorded to the nearest 0.01 mm. The tangent of the stress-strain curves at about 50% of the failure stress determines the deformation parameters. The deformation moduli (E) and Poisson's ratio (ν) are determined by from 3-D elastic equations given by (Jaeger, Cook, and Zimmerman, 2007), as follows:

$$\varepsilon_1 = \sigma_1/E_1 - \nu(\sigma_2/E_2 + \sigma_3/E_3) \quad (4.1)$$

$$\varepsilon_2 = \sigma_2/E_2 - \nu(\sigma_1/E_1 + \sigma_3/E_3) \quad (4.2)$$

$$\varepsilon_3 = \sigma_3/E_3 - \nu(\sigma_1/E_1 + \sigma_2/E_2) \quad (4.3)$$

where σ_1 is vertical stress (major principal stress), σ_2 and σ_3 are horizontal stresses (minor principal stresses), and ε_1, ε_2, and ε_3 are major, intermediate, and minor principal strains, and E_1, E_2 and E_3 are the deformation moduli along the major, intermediate and minor principal directions. Here it is assumed that the rock specimens are homogeneous, as a result, E_1, E_2 and E_3 are identical.

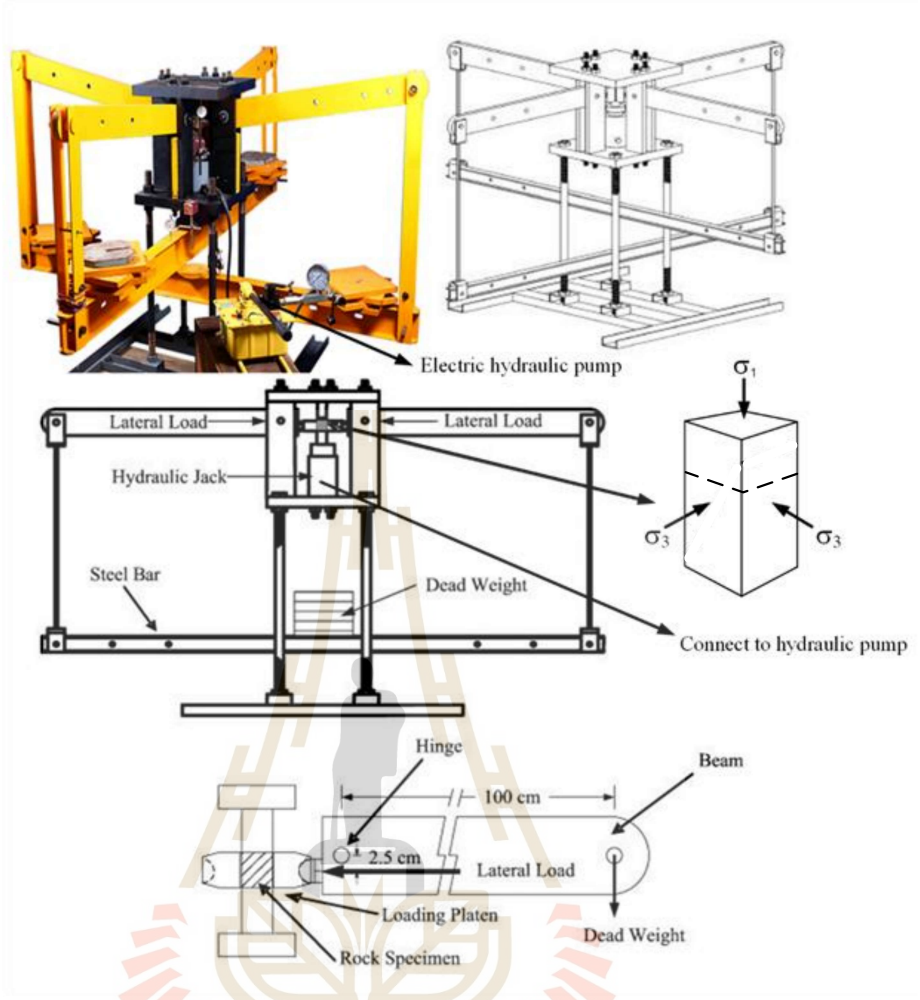

Figure 4.1 Polyaxial load frame used in single and multi-stage triaxial compression testing (Fuenkajorn et al., 2012).

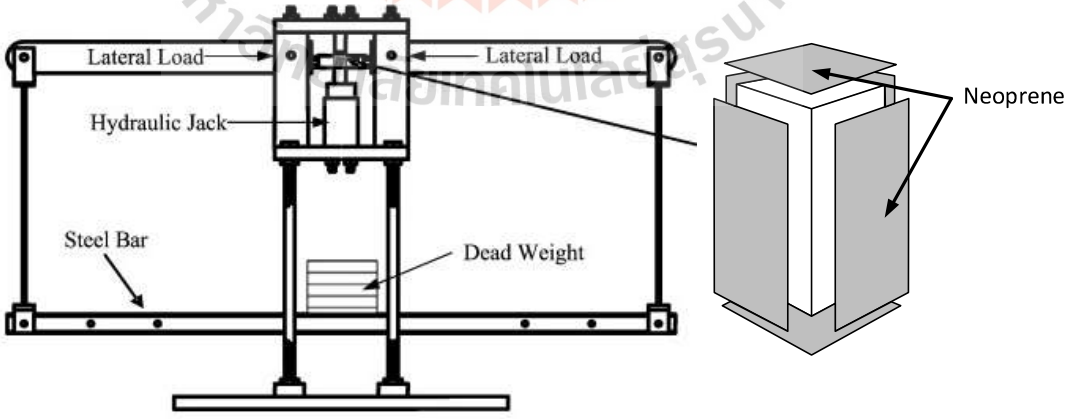

Figure 4. 2 Specimen with neoprene placed between all interfaces and loading platens in polyaxial load frame (Fuenkajorn et al., 2012).

4.3 Multi-stage triaxial compression test

The multi-stage triaxial compression testing aims to measure the maximum failure stress and axial and lateral strains during loading and reloading phases by conducting a multi-stage loading using polyaxial compression frame (Fuenkajorn, Sriapai, and Samsri, 2012). These tests are carried out under constant confining pressures between 0 and 40 MPa. The multi-stage stress path is shown in Figure 4.3. Under hydrostatic conditions, confining pressure (σ_3) and axial σ_1) stress are first simultaneously increased to the required confining pressure. The axial stress is then raised to failure and then released to the original confining pressure. Both axial and confining stresses then increased to the next level of confining pressure. After that, axial stress is once raised to reach the peak strength. This cycle is repeated to allow analysis of rock strength at various confining pressures. Axial stress and strains and lateral strains are plotted continuously from the first to the last loading stages. To find the deformation moduli (E) and Poisson's ratio (ν), the multi-stage triaxial compressive tests used reloading values of the stress–strain curve at about 50% of the failure stresses under different confining pressures. The deformation calculations used the same formulas as the single stage triaxial compressive tests method given by (Jaeger, Cook, and Zimmerman, 2007).

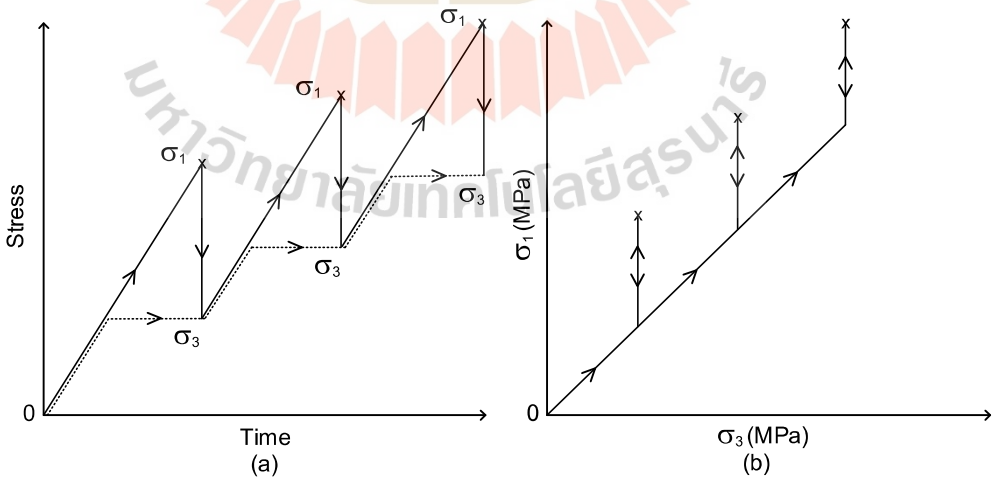

Figure 4. 3 Stress path for multi-stage triaxial compression test used in this study, (a) stress variations with time and (b) axial stress as a function of confining pressure (σ_3).

CHAPTER V
TEST RESULTS

5.1 Introduction

This chapter describes the results of single and multi-stage triaxial compression tests for all rock types. The maximum axial stresses at failure are presented for each confining pressure. The deformation moduli and Poisson's ratios are determined for both test conditions using the three-dimensional stress-strain relations given in Chapter IV. These parameters are calculated from the loading curves at 40-50% of the peak stress.

5.2 Single stage test results

The results of single stage triaxial compression tests conducted under confining pressures (σ_3) ranging from 0 to 40 MPa. They are performed to compare with the multi-stage triaxial tests. Extension failure is observed in high-loading specimens. The high confining pressures result in multiple fractures. Some post-tested single stage specimens are shown in Figure 5.1. The test results are shown as stress-strain curves in Figures 5.2. The elastic moduli and Poisson's ratio are given in Table 5.1.

5.3 Multi-stage test results

The results of multi-stage triaxial compression tests conducted under confining pressures (σ_3) ranging from 0 to 40 MPa. These tests are performed to compare with the single-stage triaxial tests. The specimens exhibit varying failure patterns depending on the applied stress level at each stage. Under confining pressure, deformation was observed to gradually increase as each subsequent step was initiated at a higher confining pressure. All post-tested multi-stage specimens are shown in Figure 5.3. The test results are presented as stress-strain curves in Figures 5.4. The elastic moduli and Poisson's ratio are given in Table 5.2.

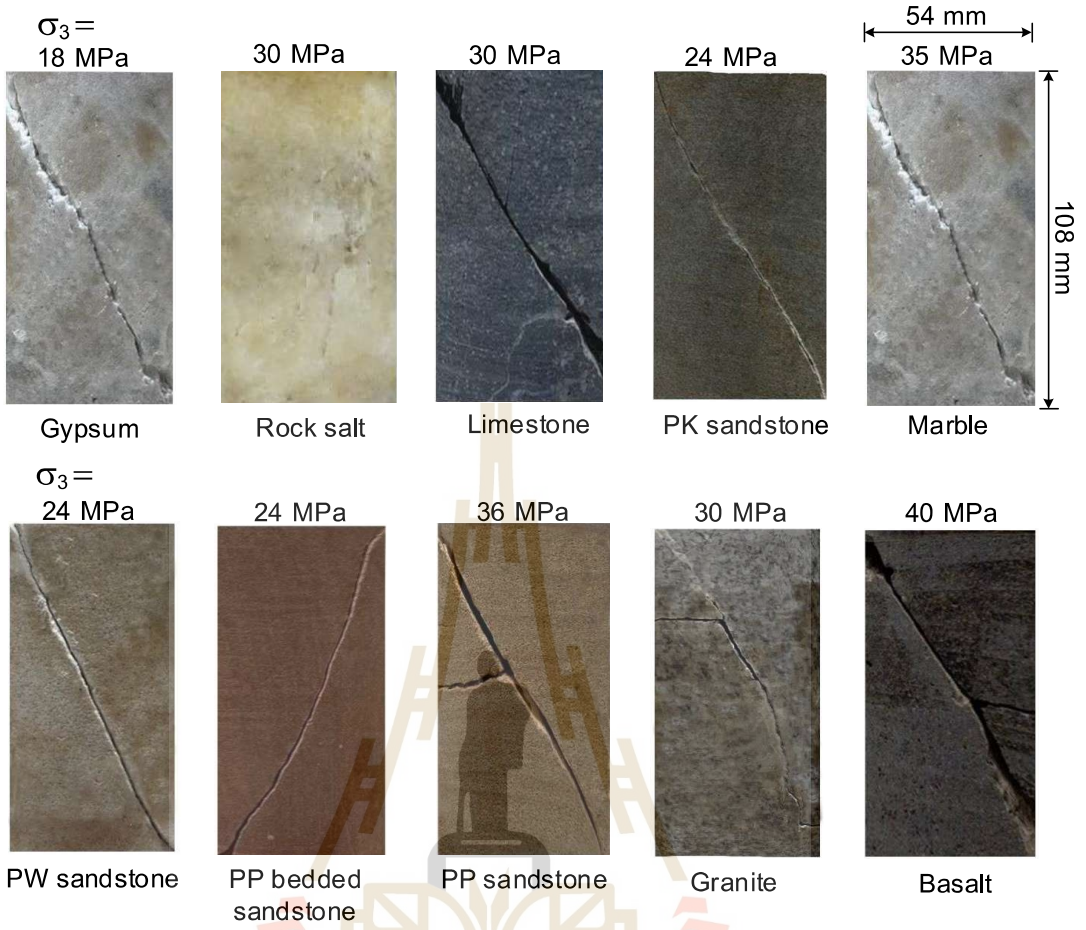

Figure 5.1 Some post-tested specimens of the single stage triaxial compression test.

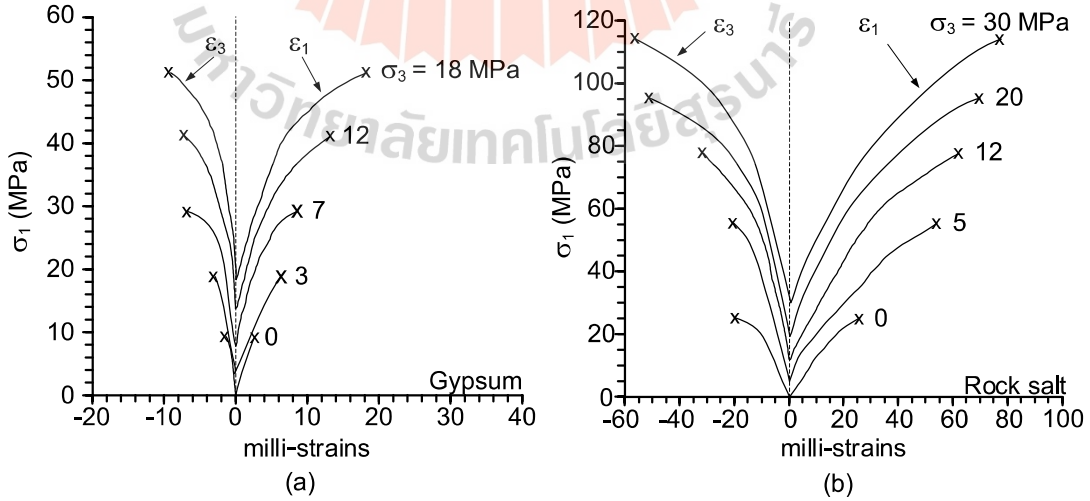

Figure 5.2 Stress-strain curves for Tak Fa gypsum (a), Maha Sarakham salt (b).

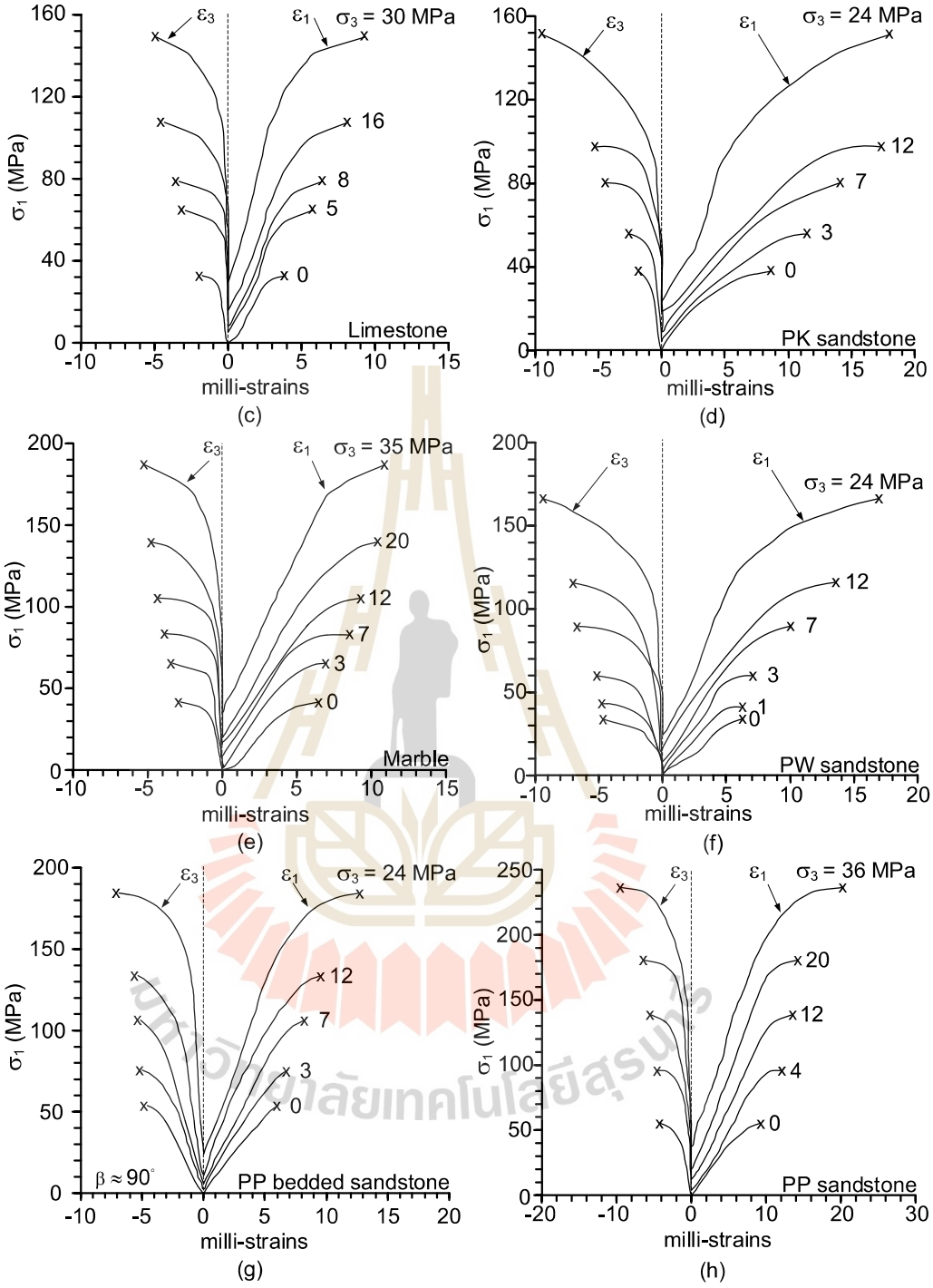

Figure 5.2 Stress-strain curves for Khao Khad bedded limestone (c), Phu Kradung sandstone (d), Khao Khad marble (e), Pha Wihan sandstone (f), Phu Phan bedded sandstone (g), Phu Phan sandstone (h). (cont.)

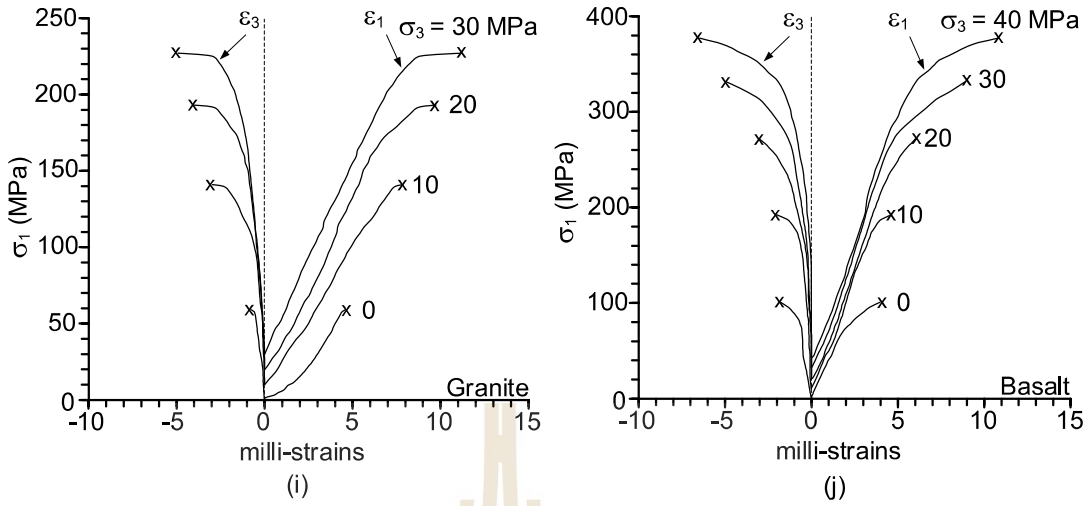

Figure 5.2 Stress-strain curves for Rayong-Bang Lamung granite (i), Buriram basalt (j). (cont.)

Table 5.1 Summary results of Young's moduli, as well as Poisson's ratios of single stage triaxial compression tests.

Rock Types	Confining pressure σ_3 (MPa)	E_s (GPa)	ν_s
Tak Fa gypsum	0	4.6	0.28
	1	-	-
	3	6.0	0.27
	7	8.6	0.26
	12	9.9	0.25
	18	11.5	0.23
Maha Sarakham salt	0	1.2	0.38
	1	-	-
	5	1.6	0.36
	12	2.1	0.33
	20	2.4	0.31
	30	2.5	0.30
Khao Khad bedded limestone	0	12.6	0.24
	1	-	-
	5	17.0	0.20
	8	18.7	0.19
	16	21.6	0.17
	30	27.7	0.15
Phu Kradung sandstone	0	6.5	0.24
	1	-	-
	3	7.2	0.20
	7	9.4	0.19
	12	10.9	0.17
	24	12.3	0.15

Table 5.1 Summary results of Young's moduli, as well as Poisson's ratios of single stage triaxial compression tests. (cont.)

Rock Types	Confining pressure σ_3 (MPa)	E_s (GPa)	ν_s
Khao Khad marble	0	11.3	0.24
	1	-	-
	3	13.3	0.22
	7	15.4	0.20
	12	16.9	0.19
	20	18.7	0.17
	35	21.8	0.15
Pha Wihan sandstone	0	10.4	0.26
	1	-	-
	3	11.3	0.24
	7	13.2	0.22
	12	15.9	0.20
	24	17.5	0.17
Phu Phan bedded sandstone	0	11.6	0.21
	1	-	-
	3	12.2	0.20
	7	12.6	0.19
	12	13.9	0.17
	24	17.2	0.15
Phu Phan sandstone	0	8.3	0.25
	1	-	-
	4	9.7	0.24
	12	12.7	0.23
	20	14.4	0.22
	36	16.9	0.19
Rayong-Bang Lamung granite	0	18.1	0.23
	1	-	-
	5	-	-
	10	20.5	0.21
	20	22.9	0.20
	30	24.6	0.18
Buriram basalt	0	38.1	0.17
	1	-	-
	10	42.6	0.16
	20	45.6	0.15
	30	48.9	0.14
	40	51.4	0.13

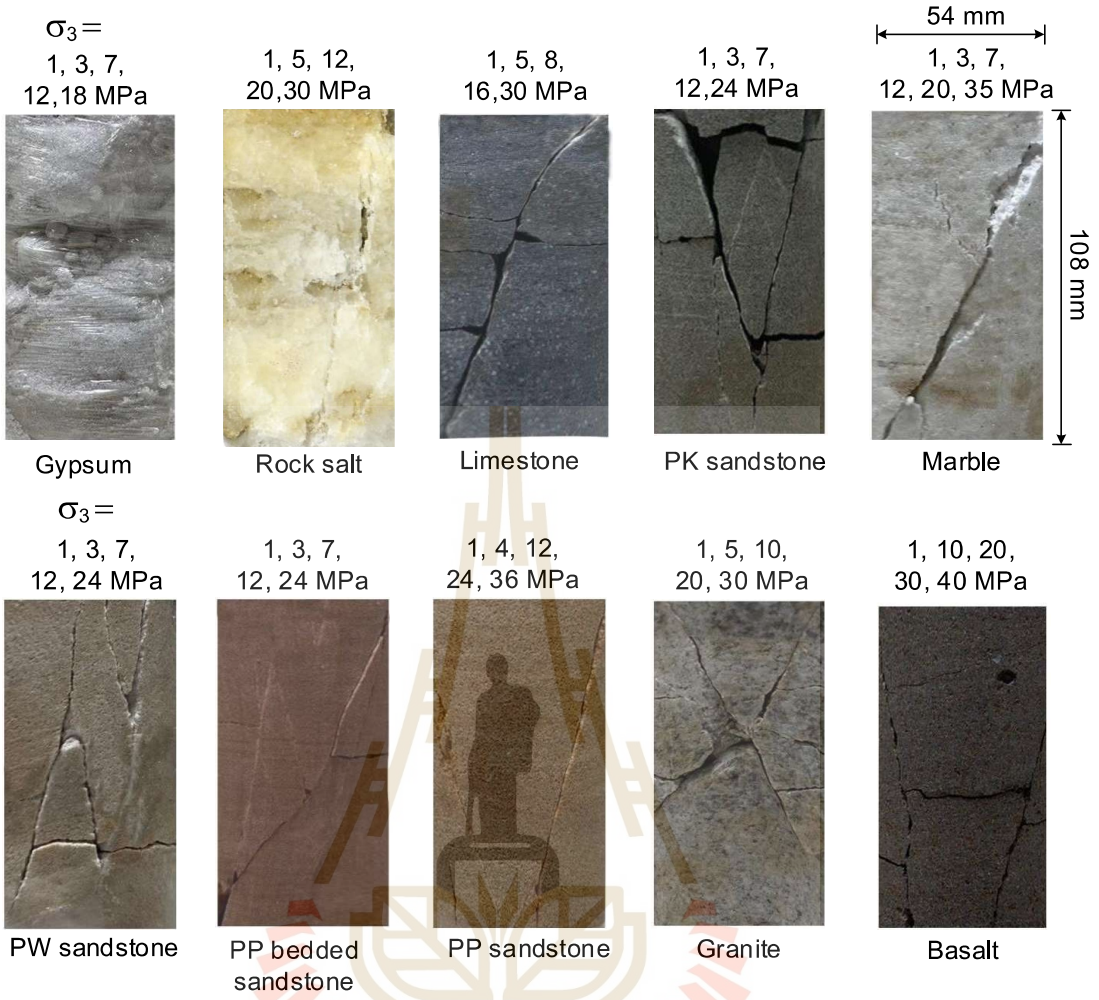

Figure 5.3 All post-tested specimens of multi-stage triaxial compression tests after confining pressure of 1, 3, 4, 5, 7, 8, 10, 12, 16, 18, 20, 24, 30, 35, 36, 40 MPa.

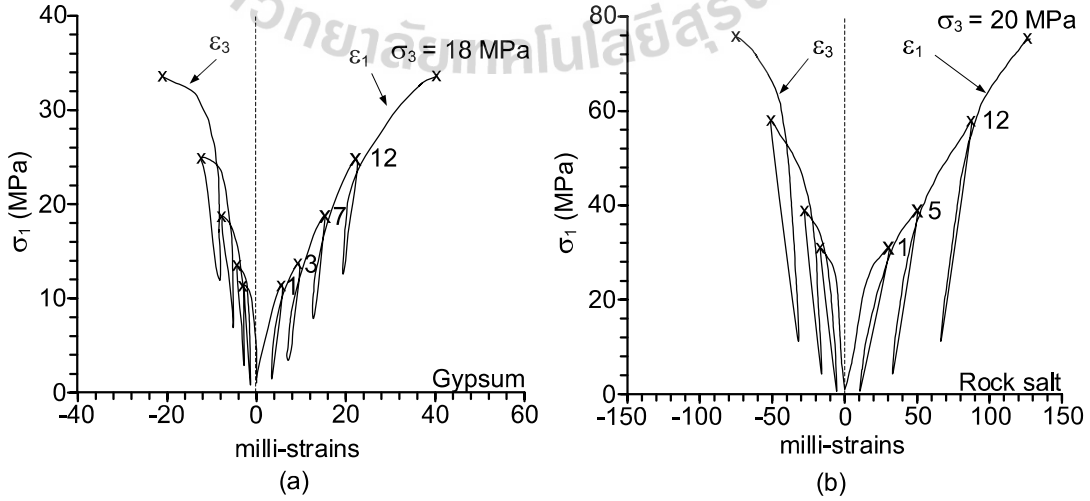

Figure 5.4 Stress-strain curves for Tak Fa gypsum (a), Maha Sarakham salt (b).

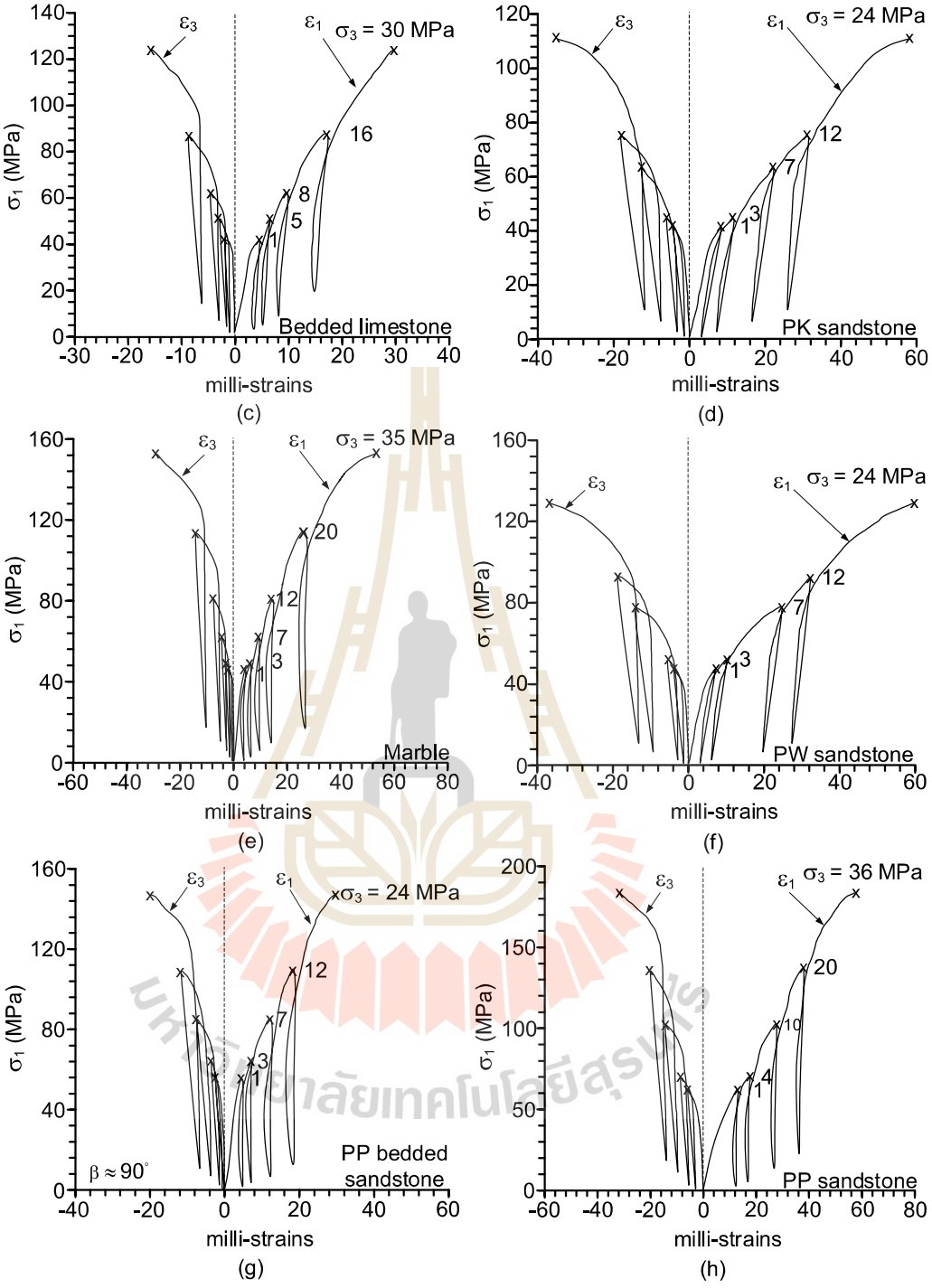

Figure 5.4 Stress-strain curves for Khao Khad bedded limestone (c), Phu Kradung sandstone (d), Khao Khad marble (e), Pha Wihan sandstone (f), Phu Phan bedded sandstone (g), Phu Phan sandstone (h). (cont.)

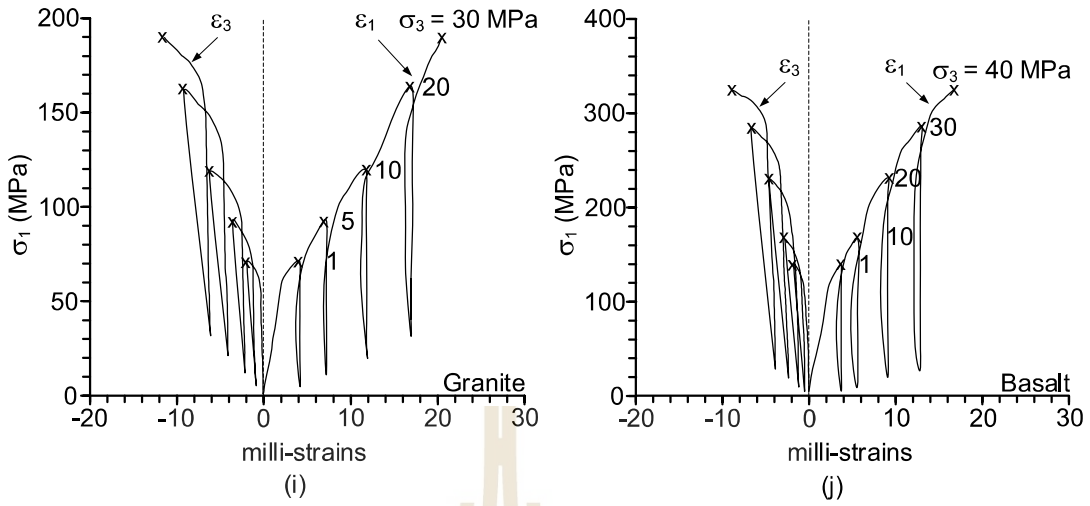

Figure 5.4 Stress-strain curves for Rayong-Bang Lamung granite (i), Buriram basalt (j). (cont.)

Table 5. 2 Summary results of Young's moduli, as well as Poisson's ratios of multi-stage triaxial compression tests.

Rock Types	Confining pressure σ_3 (MPa)	E_m (GPa)	ν_m
Tak Fa gypsum	0	-	-
	1	4.8	0.28
	3	5.9	0.29
	7	7.4	0.30
	12	8.7	0.31
	18	10.8	0.33
Maha Sarakham salt	0	-	-
	1	1.3	0.38
	5	1.4	0.39
	12	2.0	0.40
	20	2.1	0.41
	30	2.3	0.43
Khao Khad bedded limestone	0	-	-
	1	14.7	0.22
	5	16.7	0.23
	8	17.9	0.24
	16	20.2	0.25
	30	26.7	0.27
Phu Kradung sandstone	0	-	-
	1	6.7	0.23
	3	7.1	0.24
	7	9.0	0.25
	12	10.3	0.26
	24	11.8	0.28

Table 5.2 Summary results of Young's moduli, as well as Poisson's ratios of multi-stage triaxial compression tests. (cont.)

Rock Types	Confining pressure σ_3 (MPa)	E_m (GPa)	ν_m
Khao Khad marble	0	-	-
	1	11.9	0.23
	3	12.8	0.24
	7	14.7	0.25
	12	16.7	0.26
	20	17.9	0.27
	35	21.1	0.29
Pha Wihan sandstone	0	-	-
	1	10.6	0.25
	3	11.2	0.26
	7	12.7	0.27
	12	14.5	0.28
	24	17.1	0.31
Phu Phan bedded sandstone	0	-	-
	1	11.8	0.21
	3	11.9	0.22
	7	12.2	0.23
	12	13.4	0.24
	24	16.5	0.25
Phu Phan sandstone	0	-	-
	1	8.8	0.25
	4	9.7	0.26
	12	11.7	0.27
	20	12.9	0.28
	36	15.6	0.30
Rayong-Bang Lamung granite	0	-	-
	1	19.4	0.23
	5	19.9	0.24
	10	20.2	0.25
	20	22.1	0.26
	30	24.3	0.28
Buriram basalt	0	-	-
	1	41.6	0.16
	10	42.3	0.17
	20	43.8	0.18
	30	47.4	0.20
	40	50.9	0.22

CHAPTER VI
ANALYSIS OF TEST RESULTS

6.1 Introduction

The primary objective of this chapter is to determine mathematical correlations of the strengths and deformation moduli between the single and multi-stage triaxial compression tests. The findings will allow predicting the single stage test results from the multi-stage results. The correlation relations will also be applied to the multi-stage test results obtained elsewhere from other researchers.

6.2 Compressive strengths

Hoek-Brown criterion (Hoek-Brown, 1980) is applied to the triaxial compression strengths, using data obtained from both single and multi-stage test conditions, based on the compressive strengths of test results in Table 6.1. It represents the principal stresses at failure ($\sigma_{1,f}$) as (Hoek and Brown, 1980):

$$\sigma_{1,f} = \sigma_3 + (m \cdot \sigma_c \cdot \sigma_3 + s \cdot \sigma_c^2)^{1/2} \quad (6.1)$$

where σ_3 and σ_c are confining pressure and uniaxial compressive strength of rock. The parameters m and s are empirical constants. Regression analyses are performed on the test results to determine these parameters. Table 6.2 gives the analysis results for both single and multi-stage test conditions. The $\sigma_{1,f} - \sigma_3$ curves obtained from the regression are compared with the test data for all rock types in Figure 6.1. Good correlations are obtained ($R^2 > 0.9$).

6.3 Hoek-Brown parameters

An attempt is made to correlate Hoek-Brown parameters obtained from the two test conditions. Since both parameters depend on uniaxial compression strength of rocks. They are plotted as a function of σ_c in Figure 6.2.

Table 6.1 Compressive strengths of tested rocks.

Rock Types	Confining pressure σ_3 (MPa)	$\sigma_{1,f}$ (MPa)	
		Single stage	Multi-stage
Tak Fa gypsum	0	10.8	-
	1	-	11.3
	3	17.9	13.3
	7	28.3	18.1
	12	40.8	24.6
	18	51.3	33.1
Maha Sarakham salt	0	25.1	-
	1	-	27.2
	5	55.3	35.9
	12	77.1	54.1
	20	95.6	71.5
	30	114.2	89.5
Khao Khad bedded limestone	0	32.6	-
	1	-	35.2
	5	64.2	50.3
	8	78.3	61.2
	16	107.1	85.6
	30	149.1	121.5
Phu Kradung sandstone	0	38.9	-
	1	-	40.4
	3	58.0	4.37
	7	77.7	62.4
	12	97.2	73.7
	24	151.3	110.7
Khao Khad marble	0	41.7	-
	1	-	43.5
	3	65.4	50.3
	7	83.2	66.3
	12	105.2	85.3
	20	139.7	109.3
	35	186.9	147.2
Pha Wihan sandstone	0	43.3	-
	1	-	46.8
	3	63.4	51.3
	7	88.9	76.6
	12	106.9	91.3
	24	166.4	129.0
Phu Phan bedded sandstone	0	53.7	-
	1	-	55.3
	3	78.3	63.5
	7	105.4	84.6
	12	130.2	108.4
	24	186.5	144.9
Phu Phan sandstone	0	55.0	-
	1	-	57.2
	4	95.7	75.3
	12	138.8	110.5
	20	180.4	147.3
	36	235.9	195.3
Rayong-Bang Lamung granite	0	59.1	-
	1	-	61.0
	5	-	86.2
	10	140.3	115.4
	20	191.3	157.4
	30	225.3	191.9
Buriram basalt	0	100.6	-
	1	-	107.3
	10	192.1	175.3
	20	271.2	240.5
	30	331.9	290.3
	40	376.5	325.4

Table 6.2 Hoek-Brown parameters obtained from single and multi-stage strength results.

Rock Types	Parameters	Single stage	Multi-stage
Tak Fa gypsum	m	5.01	0.88
	s	1.00	0.57
	R^2	0.995	0.998
Maha Sarakham salt	m	9.94	3.89
	s	1.00	0.62
	R^2	0.978	0.995
Khao Khad bedded limestone	m	13.92	7.18
	s	1.00	0.64
	R^2	0.998	0.999
Phu Kradung sandstone	m	14.32	7.37
	s	1.00	0.65
	R^2	0.991	0.992
Khao Khad marble	m	14.66	7.55
	s	1.00	0.68
	R^2	0.999	0.998
Pha Wihan sandstone	m	15.93	8.53
	s	1.00	0.71
	R^2	0.989	0.993
Phu Phan bedded sandstone	m	17.92	9.70
	s	1.00	0.73
	R^2	0.999	0.995
Phu Phan sandstone	m	19.58	11.31
	s	1.00	0.75
	R^2	0.996	0.998
Rayong-Bang Lamung granite	m	20.60	12.96
	s	1.00	0.77
	R^2	0.996	0.999
Buriram basalt	m	26.00	19.14
	s	1.00	0.83
	R^2	0.998	0.996

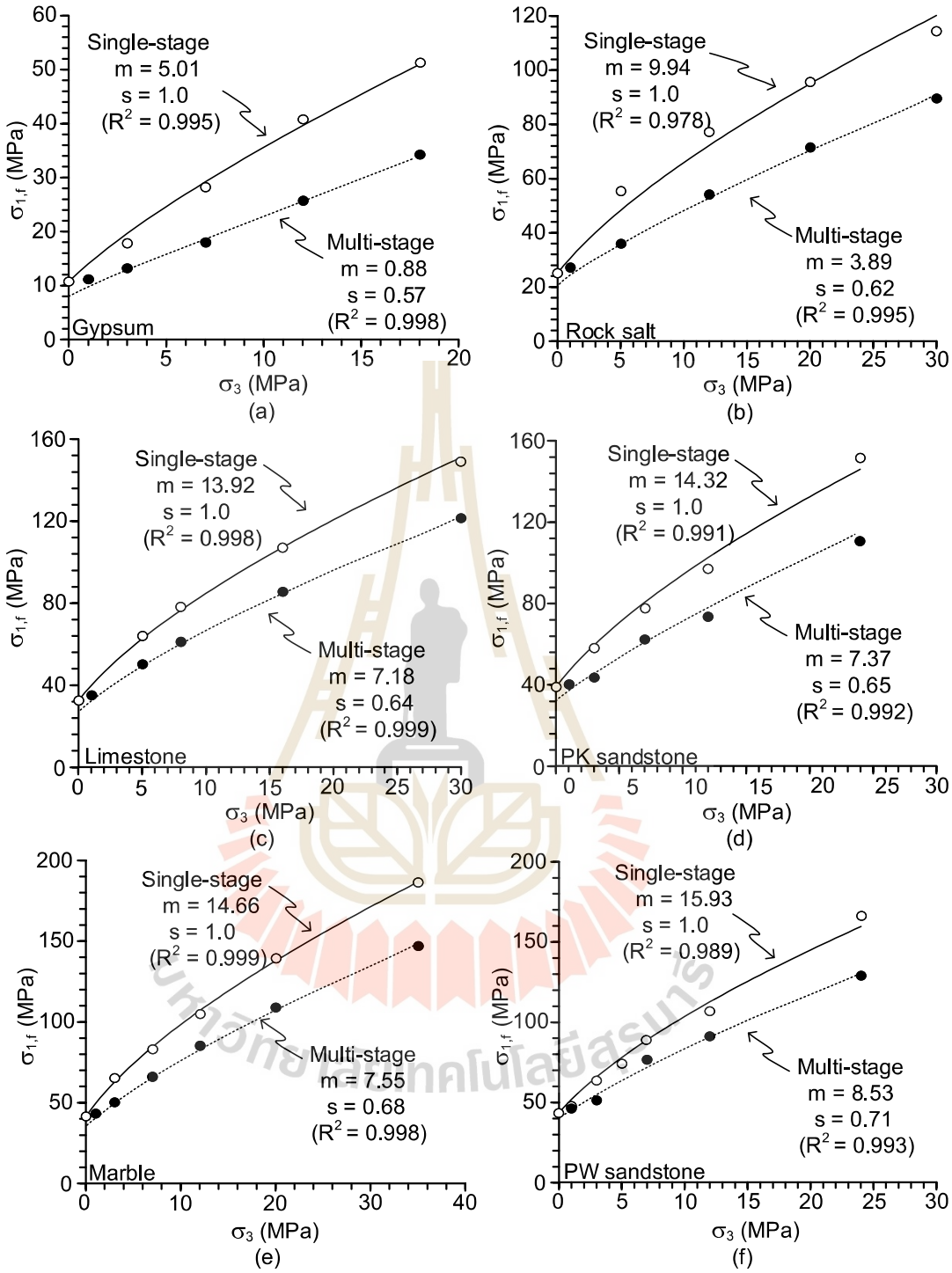

Figure 6.1 Compressive strengths at failure as a function of confining pressure for Tak Fa gypsum (a), Maha Sarakham salt (b), Bedded limestone (c), Phu Kradung sandstone (d), Khao Khad marble (e), Pha Wihan sandstone (f).

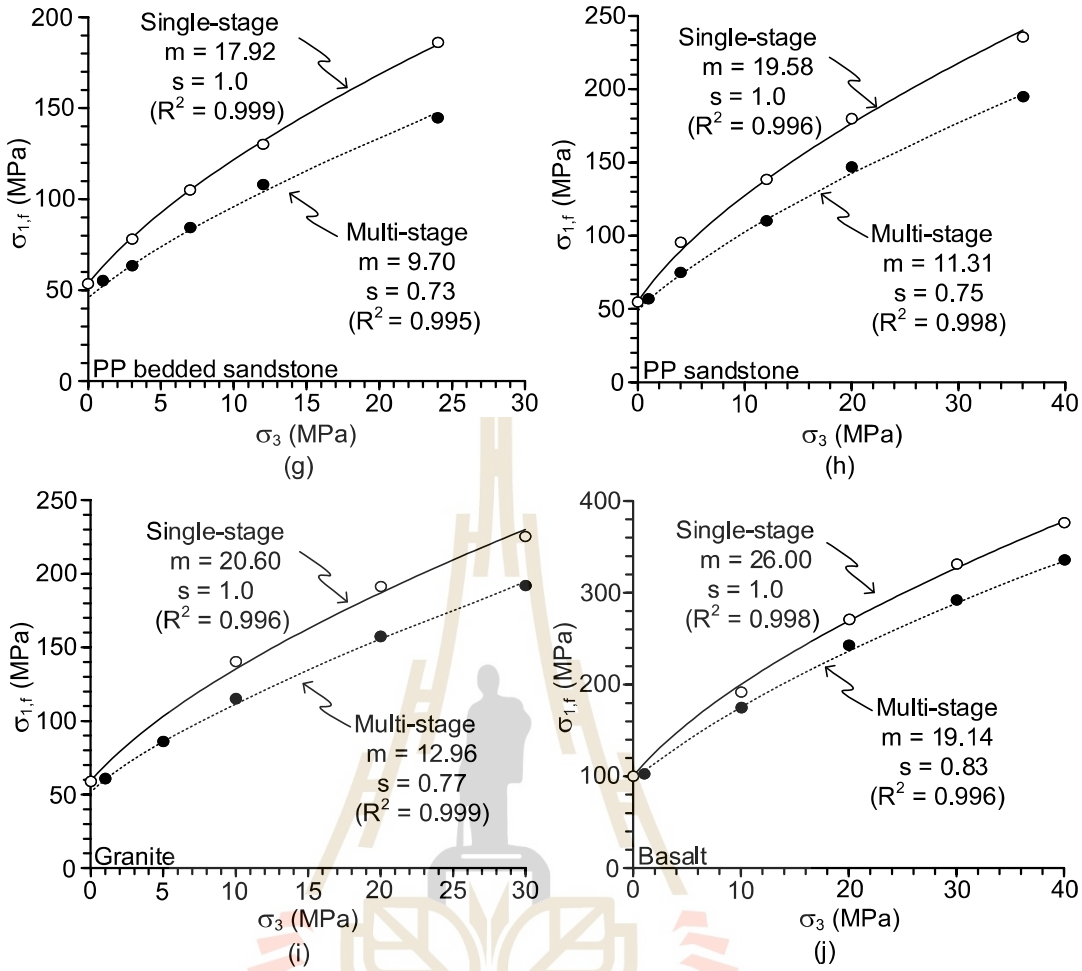

Figure 6.1 Compressive strengths at failure as a function of confining pressure for Phu Phan bedded sandstone (g), Phu Phan sandstone (h), Rayong-Bang Lamung granite (i), Burirum basalt (j). (cont.)

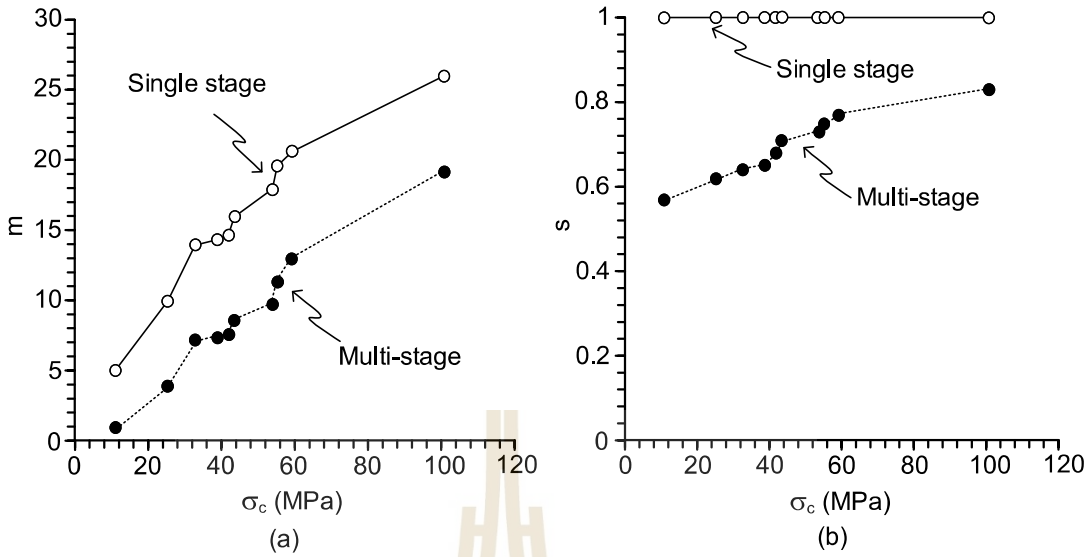

Figure 6.2 Hoek-Brown parameters, m (a), and s (b) as a function of uniaxial compressive strength (σ_c).

The parameter m increases with σ_c. where single stage test condition gives higher values than the multi-stage condition. The parameter s for the single stage test is equal to one for all rock types as it is calibrated from the intact rocks. For multi-stage testing however parameter s shows the values of less than one. The weaker rocks give the lower s values than the stronger rocks (higher σ_c).

To correlate the Hoek-Brown parameters between the two test conditions, the subscript m denoting multi-stage is assigned for the multi-stage parameters (m_m and s_m), where subscript s (denoting single stage) is using for the single stage parameters (m_s and s_s). After several trials, ratios of the Hoek-Brown parameters are proposed as: m_m/m_s and s_m/s_s. They are plotted in Figure 6.3.

Exponential equations are fitted to these ratios. Good correlation is obtained. They can be presented as:

$$m_m/m_s = 1 - a \cdot \exp(-b \cdot \sigma_c) \quad (6.2)$$

$$s_m/s_s = 1 - c \cdot \exp(-d \cdot \sigma_c) \quad (6.3)$$

when a, b, c, d are empirical constants. The m_m/m_s ratio allows predicting then m_s value for single stage testing of the m_m value is known for the multi-stage testing. Extrapolation of the two equations above allows predicting the uniaxial compressive strengths of rocks at which the m_m/m_s and s_m/s_s approach one are given in Table 6.3.

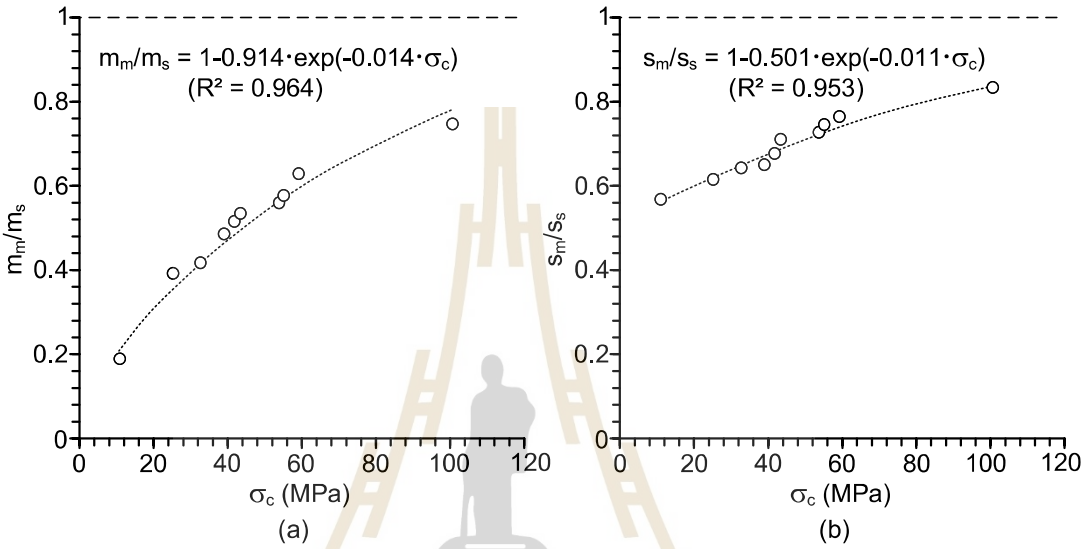

Figure 6.3 Relationships between m_m/m_s ratios (a), and s_m/s_s ratios (b) as a function of uniaxial compressive strength (σ_c).

Table 6.3 m_m/m_s and s_m/s_s ratios obtained from single and multi-stage strength results.

Rock Types	m_m/m_s	s_m/s_s
Tak Fa gypsum	0.19	0.57
Maha Sarakham salt	0.39	0.62
Khao Khad bedded limestone	0.42	0.64
Phu Kradung sandstone	0.43	0.65
Khao Khad marble	0.51	0.68
Pha Wihan sandstone	0.54	0.71
Phu Phan bedded sandstone	0.56	0.73
Phu Phan sandstone	0.58	0.75
Rayong-Bang Lamung granite	0.63	0.77
Buriram basalt	0.74	0.83

6.4 Strengths from researches obtained elsewhere

Figure 6.4 compares the m_m/m_s ratio obtained from this study with those published by other researches who conduct both multi-stage and single stage compression testing on various rock types. The solid points in the diagram represent the results obtained from the same loading path are used in this study. The open data points are those from different loading paths of multi-stage testing. The error between the prediction and the results obtained elsewhere are calculated using equations as follows (Khair, Fahmi, Al Hakim, and Rahim, 2017):

$$\text{Error} = 1/n \sum_{i=1}^{n} \left| m_m/m_{s\,(i,\,p)} - m_m/m_{s\,(i,\,t)} \,/\, m_m/m_{s\,(i,\,p)} \right| \cdot 100 \qquad (6.4)$$

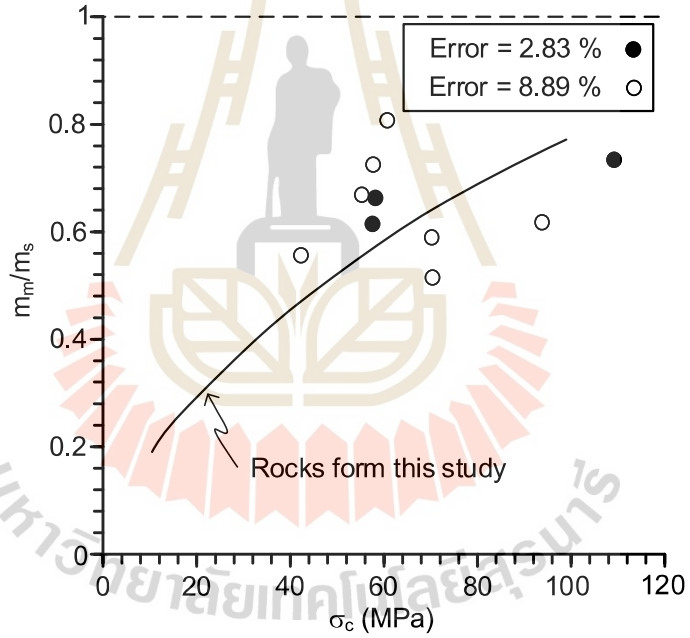

Figure 6.4 Solid points are results from Yang et al. (2012). Open points are from others: Aghababaei et al. (2019), Shi et al. (2016), Venter et al. (2016), Cain et al. (1986).

6.5 Deformation moduli

Figure 6.5 plots the elastic or deformation moduli as a function of confining pressure (σ_3), where E_m and E_s represent the values obtained from multi-stage and single stage testing. Both increase with confining pressure, where the single stage testing gives higher values than those from multi-stage tests. The Poisson's ratios from both test conditions are also presented as a function of confining pressure in Figure 6.6. They are denoted by ν_s for single stage and ν_m for multi-stage. The single stage testing shows the decrease of ν_s as σ_3 increases, while the multi-stage testing shows the increase of ν_m with σ_3. This is probably due to the accumulation of the induced fractures in the specimens as the loading cycles increase.

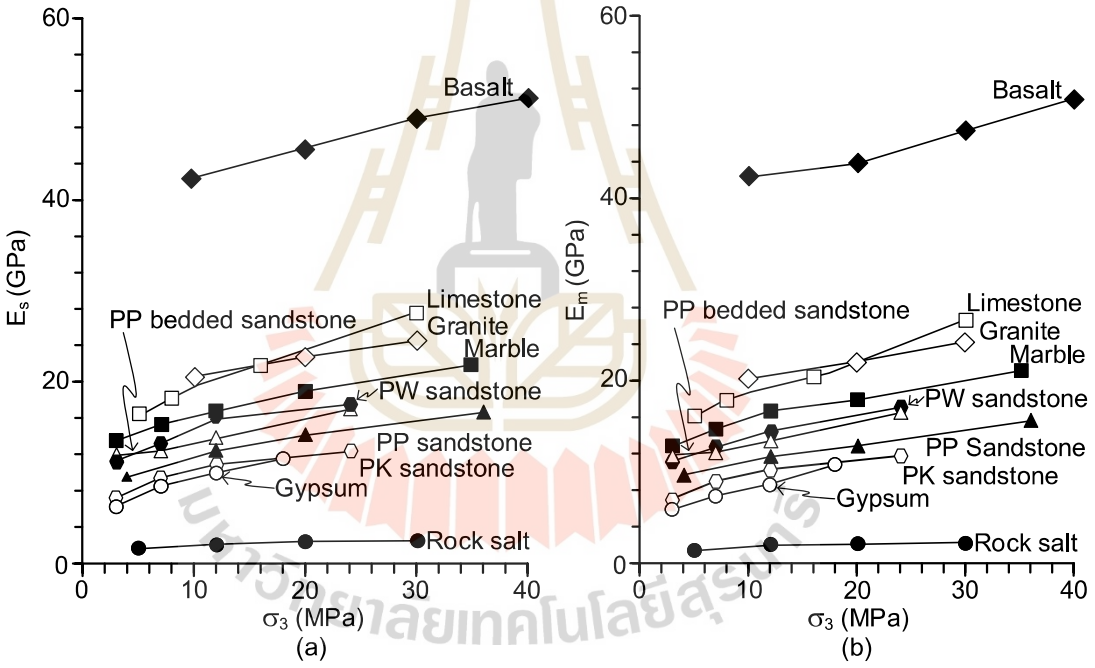

Figure 6.5 Elastic moduli for single stage, E_s (a), and multi-stage, E_m (b), as a function of confining pressure (σ_3).

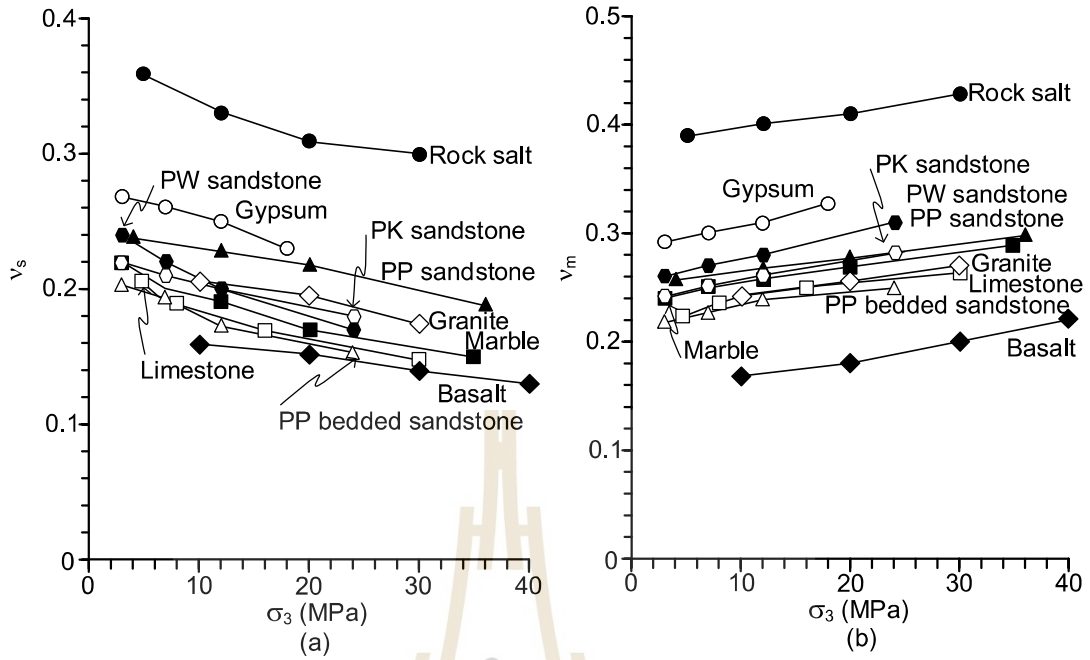

Figure 6.6 Poisson's ratios for single stage, ν_s (a), and multi-stage, ν_m (b), as a function of confining pressure (σ_3).

To correlate the deformation moduli obtained between both test conditions, empirical equation are proposed as:

$$\frac{1}{E_m} = \frac{1}{E_s} + \frac{1}{\beta} \tag{6.6}$$

$$\frac{1}{G_m} = \frac{1}{G_s} + \frac{1}{\alpha} \tag{6.7}$$

where E_m is elastic moduli obtained from multi-stage, E_s is elastic moduli obtained from single stage, G_m and G_s are shear moduli obtained from multi-stage and single stage testing ($G = E/2(1+\nu)$). The parameters β and α are empirical constants correlating the two test conditions. Their numerical values are obtained from regression analysis and are given in Table 6.4.

To allow predicting the multi-stage deformation and shear moduli for different rock types, the constants β and α are correlated with the uniaxial compressive strength of the rocks tested here. Figure 6.7 plots these constants as a function of σ_c. Exponential equation is proposed to represent their variations with the evolution of σ_c, as follows:

$$\beta = 1 + 98.85 \cdot \exp(0.027 \cdot \sigma_c) \quad (6.7)$$

$$\alpha = 1 + 15.39 \cdot \exp(0.029 \cdot \sigma_c) \quad (6.8)$$

The numerical values in the equations are obtained from regression analysis. Good correlations are obtained ($R^2 > 0.8$). If σ_c of any rock is known, constants β and α can be determined, and subsequently E_s and G_s can be predicted from E_m and G_m. They can be substituted in equations (6.7 and 6.8) to predict the deformation and shear moduli of single stage testing from the results of multi-stage testing.

Table 6.4 Empirical constants β and α.

Rock Types	β (GPa)	α (GPa)
Tak Fa gypsum	0.072	0.021
Maha Sarakham salt	0.018	0.004
Khao Khad bedded limestone	0.431	0.080
Phu Kradung sandstone	0.228	0.045
Khao Khad marble	0.431	0.065
Pha Wihan sandstone	0.223	0.050
Phu Phan bedded sandstone	0.402	0.065
Phu Phan sandstone	0.150	0.038
Rayong-Bang Lamung granite	0.854	0.122
Buriram basalt	1.490	0.286

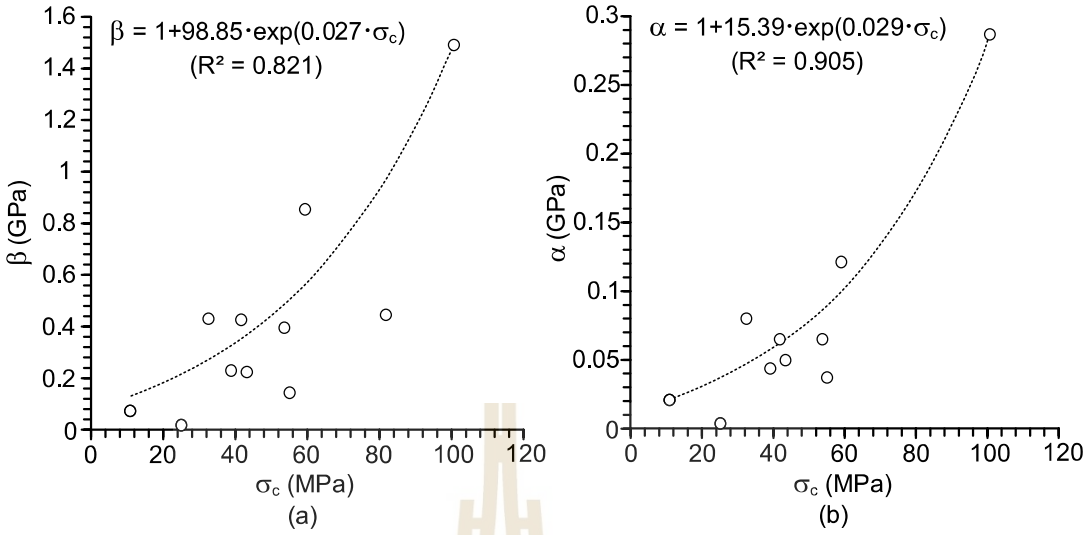

Figure 6.7 Constants β (a), and α (b) as a function of uniaxial compressive strength (σ_c).

CHAPTER VII
DISCUSSIONS AND CONCLUSIONS

This chapter discusses the adequacy of the test results and the scope, limitations and applications of the mathematical correlations between single and multi-stage triaxial compression testing. Conclusions drawn from the test results and analysis are also presented.

7.1 Discussions

Due to the fact that the $\sigma_{1,f} - \sigma_3$ relations for all tested rocks are not linear, as shown in Figure 6.1, the conventional Coulomb strength criterion is not applicable here. In addition, the criterion is only for intact rock specimens, and hence it is not valid for the multi-stage testing specimens where they are failed after the first loading cycle. Hoek-Brown criterion seems more appropriate for this study as it is capable of describing the compressive strengths of the intact specimens for the single stage tests and the failed specimens for multi-stage testing.

Rock types selected for this study have uniaxial compressive strengths ranging from soft rock (gypsum – 10.8 MPa) to strong rock (basalt – 100.6 MPa). This allows deriving an appropriate mathematical relations between m_m/m_s ratios and the strength (i.e., Equation (6.2)). Missing from this study is the very strong rock specimens ($\sigma_c > 250$ MPa), as they are rarely encountered in the geo-engineering projects and mines in Thailand.

Good correlations between m_m/m_s ratio and σ_c and between s_m/s_s ratio and σ_c support that the triaxial compression strengths for the single stage testing that uses several specimens to accomplish can be predicted by the results of the multi-stage testing that uses much fewer specimens. As a minimum the multi-stage testing requires only one uniaxial compression test to obtain σ_c and one multi-stage triaxial testing to obtain m_m and s_m. The three parameters can be used to predict m_s and s_s (always equals to 1) for the single stage testing.

Comparison of the correlation equation obtained from this study with the multi-stage strength results obtained elsewhere by other researchers suggests that the multi-stage strengths are sensitive to the loading path. If a multi-stage testing uses the same loading path that used here the prediction by equation (6.2) can give good correlation with the error of about 2.83%, as shown in Figure 6.4. For multi-stage strengths obtained under different loading paths (i.e., not allowing axial stress to drop from the failure stress to the current confining pressure), as performed by Shi et al. (2016) and Venter, Purvis, and Hamman (2016) and Cain, Yuen, Le Bel, Crawford, and Lau (1986), larger error can be obtained, as shown in Figure 6.4.

Correlations between deformation parameters obtained from multi-stage testing (E_m and G_m) and from single stage testing as performed in this study have never been attempted elsewhere. This is due to the fact that the conventional triaxial cell or Hoek cell with strain gages or clip gages cannot measure the lateral deformations after the specimens have been failed by the first loading cycle. This study uses the polyaxial load frame that allows measuring the lateral deformations by the movement of the four cantilever beams. As a results, comparison of the deformation parameters can not be performed against the results obtained elsewhere. In another word, no one has ever measured the deformation moduli and Poisson's ratios from the multi-stage testing.

Figure 6.6 shows that the Poisson's ratios for all tested rocks decrease with increasing the confining pressures. This behavior has long been observed from other triaxial compression tests. For the multi-stage testing, however, the Poisson's ratios increase with confining pressures. This is due to that the failing specimens are dilated laterally as the loading cycles progress. It also suggests that the dilatation effect is predominant over the increased confining pressures. Note that the correlations of the elastic moduli and shear moduli (e.g., equations (6.5) and (6.6)) have similar form of that proposed by Goodman (1970). However, the parameters E_m and G_m denoted here do not represent those of rock mass as proposed by Goodman.

7.2 Conclusions

Test results and analyses performed in this study can be concluded as follows.

1) Hoek-Brown criterion can be used to correlate the triaxial compressive strengths between single and multi-stage testing.

2) Good correlation between m_m/m_s ratio and uniaxial compressive strength allows predicting the conventional single stage triaxial compressive strengths from the multi-stage compressive strength results.

3) The multi-stage triaxial strengths are sensitive to the loading paths used for each loading cycle. Different sets of compressive strengths would likely be obtained under different loading paths.

4) Polyaxial load frame allows measuring the axial and lateral deformations of the failed specimens from the multi-stage testing. As a result the deformation moduli and Poisson's ratios of the multi-stage test condition can be determined.

5) The elastic moduli, E_m and E_s, and shear moduli, G_m and G_s, can be correlated using equations with similar form of Goodman (1970) for intact and rock mass relation. This allows predicting the deformation parameters of single stage test conditions for the intact rocks from the multi-stage test condition for the failing rocks.

7.3 Recommendations for future studies

The limitations of the numbers of tested rocks used in this study load to the following recommendations for future study, as follows:

1) More rocks with a variety of strengths should be tested, in particular for those with uniaxial compressive strengths of greater than 150–250 MPa. This could enhance the predictive capability of the proposed correlation equations.

2) The effect of loading path remains poorly understanding. More tests should be conducted under different loading paths using the same sets of test specimens.

3) Numerical analysis approach is desirable to study the failure behavior of the specimens after the first cycles of the multi-stage triaxial compression test. The results could reveal how the modes of failure of rocks induced for different strengths.

4) The effect of the range and interval of the confining pressures should be studied. The could be useful to determine the appropriate ranges of confining pressure for different strengths of rocks.

REFERENCES

Aghababaei, M., Behnia, M., & Moradian, O. (2019). Experimental investigation on strength and failure behavior of carbonate rocks under multistage triaxial compression. *International Journal of Rock Mechanics and Mining Sciences*, *123*, 104099.

Al-Ajmi, A. M., & Zimmerman, R. W. (2005). Relation between the Mogi and the Coulomb failure criteria. *International Journal of Rock Mechanics and Mining Sciences*, *42*(3), 431-439.

Al-Maamori, H. M. S., El Naggar, M. H., & Micic, S. (2019). Wetting effects and strength degradation of swelling shale evaluated from multistage triaxial test. *Underground Space*, *4*(2), 79-97.

Amann, F., Kaiser, P., & Button, E. A. (2012). Experimental study of brittle behavior of clay shale in rapid triaxial compression. *Rock Mechanics and Rock Engineering*, *45*, 21-33.

ASTM D7012-14e1 (2014). Standard Test Methods for Compressive Strength and Elastic Moduli of Intact Rock Core Specimens under Varying States of Stress and Temperatures, ASTM International, West Conshohocken, PA.

Cain, P., Yuen, C. M., Le Bel, G. R., Crawford, A. M., & Lau, D. H. (1987). Triaxial testing of brittle sandstone using a multiple failure state method. *Geotechnical Testing Journal*, *10*(4), 213-217.

Crawford, A. M., & Wylie, D. A. (1987). A modified multiple failure state triaxial testing method. In *ARMA US Rock Mechanics/Geomechanics Symposium* (pp. 87-133).

Fuenkajorn, K., Sriapai, T., & Samsri, P. (2012). Effects of loading rate on strength and deformability of Maha Sarakham salt. *Engineering Geology*, *135*, 10-23.

Goodman, R.E. (1970). The deformability of joints, determination of the in situ modulus of deformation of rock. ASTM STP 447, *American Society for Testing and Materials* (pp. 174-196).

Hamza, O., Stace, R., & Reddish, D. (2005). A study of the effect of strain rate on stiffness and strength in silty mudstone using multistage triaxial testing. *Post-Mining 2005* (pp. 16-17).

Hoek, E., & Brown, E.T. (1980). *Underground excavation in rock: Institution of Mining and Metallurgy*.

Hoek, E., & Brown, E.T. (1997). Practical estimates of rock mass strength. *International Journal of Rock Mechanics and Mining Sciences*, *34*(8), 1165–1186.

Jaeger, J.C., Cook, N.G.W., & Zimmerman, R.W. (2007). *Fundamentals of rock mechanics*. 4th ed. Oxford: Blackweel.

Kaiser, P. K., & Kim, B. H. (2008). Rock mechanics challenges in underground construction and mining. *Proceedings of the First Southern Hemisphere International Rock Mechanics Symposium* (pp. 23–38). Perth: ACG. doi: 10.36487/ACG_repo/808_83.

Khair, U., Fahmi, H., Al Hakim, S., & Rahim, R. (2017). Forecasting error calculation with mean absolute deviation and mean absolute percentage error. *Journal of physics: Conference series*, *930*(1), 012002.

Kim, M. M., & Ko, H. Y. (1979). Multistage triaxial testing of rocks. *Geotechnical Testing Journal*, *2*(2), 98-105.

Kovári, K., & Tisa, A. (1975). Multiple failure state and strain controlled triaxial tests. *Rock mechanics*, *7*, 17-33.

Kovari, K., Tisa, A., Einstein, H. H., & Franklin, J. A. (1983). Suggested methods for determining the strength of rock materials in triaxial compression: revised version. *International Journal of Rock Mechanics and Mining Sciences & Geomechanics* [Abstracts]. *20*(6), 283-290.

Melati, S., Wattimena, R. K., Kramadibrata, S., Simangunsong, G. M., & Sianturi, R. G. (2014). Stress paths effects on multistage triaxial test. *ISRM International Symposium-Asian Rock Mechanics Symposium* (pp. ISRM-ARMS8).

Minaeian, V., Dewhurst, D. N., & Rasouli, V. (2020). An investigation on failure behaviour of a porous sandstone using single-stage and multi-stage true triaxial stress tests. *Rock Mechanics and Rock Engineering*, *53*, 3543-3562.

Prayanto, D. T. A., Nurhandoko, E. B. B., & Sunardi, E. (2022). Measurement of multi-stage triaxial compression test and static elastic parameters of shale samples from the Talangakar formation for a feasibility study of shale gas in the South Palembang sub-basin, South Sumatra. *Journal of Physics: Conference Series*, *2243*(1), 012020.

Shia, X., Liua, L., Menga, Y., Maoa, S., Wanga, W., Wua, J., & Wena, C. (2016). Correction model for strength parameters of a multistage triaxial compression test on sandstone. *Proceedings of the First Southern Hemisphere International Rock Mechanics Symposium* (pp. ISRM-ARMS9).

Thaweeboon, S., Dasri, R., Sartkaew, S., & Fuenkajorn, K. (2017). Strength and deformability of small-scale rock mass models under large confinements. *Bulletin of Engineering Geology and the Environment*, *76*, 1129-1141.

Tsoi, P. A., & Homenok, I. P. (2017). Study of deformation-strength properties of sandstone under multistage triaxial compression. *Journal of Physics: Conference Series*, *894*(1), 012104.

Venter, J., Purvis, C., & Hamman, J. (2016). Hoek–Brown mi estimation a comparison of multistage triaxial with single stage triaxial testing. *Proceedings of the First Asia Pacific Slope Stability in Mining Conference*. Australian Centre for Geomechanics (pp. 289-299). Perth: ACG. doi: 10.36487/ACG_rep/1604_15_Venter.

Vergara, M. R., Kudella, P., & Triantafyllidis, T. (2015). Large scale tests on jointed and bedded rocks under multi-stage triaxial compression and direct shear. *Rock Mechanics and Rock Engineering*, *48*, 75-92.

Wang, G., Feng, X. T., Yang, C., Han, Q., & Kong, R. (2022). Experimental study of the mechanical characteristics of jinping marble under multi-stage true triaxial compression testing. *Rock Mechanics and Rock Engineering*, *55*(2), 953-966.

Yang, S. Q., Ni, H. M., & Wen, S. (2014). Spatial acoustic emission evolution of red sandstone during multi-stage triaxial deformation. *Journal of Central South University*, *21*(8), 3316-3326.

Yang, S. Q., Tian, W. L., Jing, H. W., Huang, Y. H., Yang, X. X., & Meng, B. (2019). Deformation and damage failure behavior of mudstone specimens under single-stage and multi-stage triaxial compression. *Rock Mechanics and Rock Engineering*, *52*, 673-689.

Yang, S.-Q. (2012). Strength and deformation behavior of red sandstone under multi-stage triaxial compression. *Canadian Geotechnical Journal*, *49*(6), 694-709.

Youn, H., & Tonon, F. (2010). Multi-stage triaxial test on brittle rock. *International Journal of Rock Mechanics and Mining Sciences*, *47*(4), 678-684.

APPENDIX
LIST OF PUBLICATION

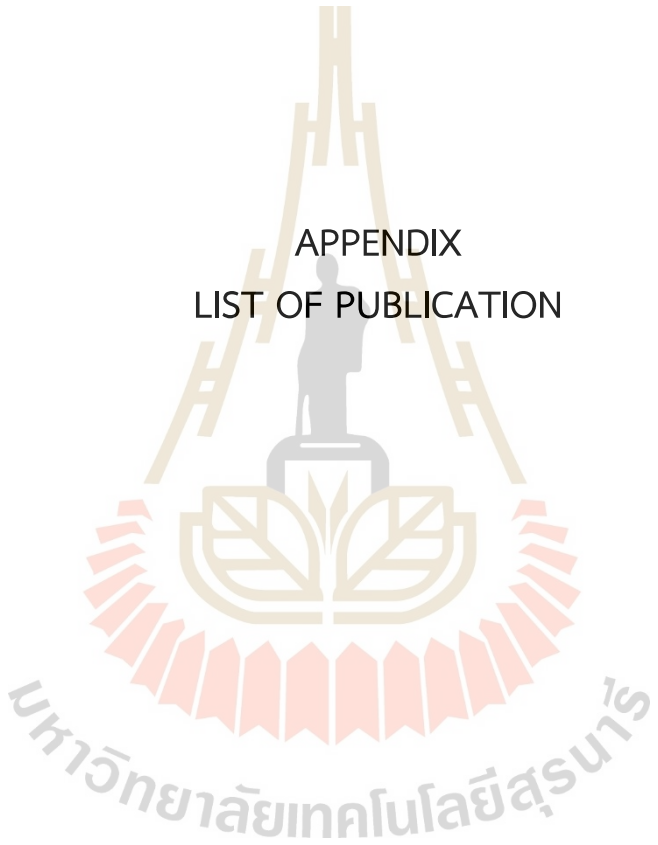

COMPARISON BETWEEN SINGLE AND MULTI-STAGE TRIAXIAL COMPRESSIVE STRENGTHS OF SOME ROCK TYPES

[1]THANAWAT SASEN, [1]KITTITEP FUENKAJORN

[1]Geomechanics Research Unit, Suranaree University of Technology, Nakhon Ratchasima, 30000, Thailand
Email: [1]M6601294@g.sut.ac.th

Abstract: This study aims at correlating the triaxial compressive strengths obtained from multi-stage testing with those from the conventional single stage test condition. Results from ten rock types are used to determine Hoek-Brown parameters under confining pressures ranging from 0 to 40 MPa. The ratio of Hoek-Brown parameters obtained from multi-stage testing to that of single stage testing (i.e. m_m/m_s) can correlate well with the rock uniaxial compressive strengths (with $R^2 > 0.9$) using an exponential equation. As a result, the triaxial compressive strength of rock can be closely predicted providing that the Hoek-Brown parameters from multi-stage testing and the uniaxial compressive strengths of the rock are known. The correlation of the strength results between the two test conditions however strongly depends on the loading path used during the multi-stage testing. Different loading paths would likely result in a different m_m/m_s–σ_c relation.

Keywords: Hoek-Brown criterion, Strength criteria, Multi-stage triaxial testing,

1. INTRODUCTION

The triaxial compression test (ASTM D7012-14) [1] has been widely used to determine rock strength and deformation under confinement, which are important parameters for the design and stability study of geological structures in civil as well as mining engineering works, including foundations for dams, structures, and bridges, and additional host rocks for underground mining and tunnels. The triaxial compression test is used in the laboratory to simulate these structures. A significant limitation of the traditional triaxial test method is that it is expensive, time-consuming, and requires a large number of standard samples. The multi-stage triaxial compression test ([2], [3] and [4]) is more popular nowadays because it requires fewer samples to determine the triaxial strength. It is found that the multi-stage strength is often lower than the single stage strength. The differences and representativeness of the multi-stage test results and the deformation modulus however require more investigation.

The multi-stage triaxial test concept was first introduced in the mid-1970s [5]. It is necessary to test a variety of rocks to conduct a comparative study of the single stage and multi-stage strengths. Accurate lateral and axial stresses of the specimen are typically difficult to measure due to non-uniform deformations of the specimen and local strain measurement by measuring equipment [6].

The objective of this study is to develop mathematical correlations between single stage and multi-stage triaxial compressive test results in terms of strength and deformability. Hoek-Brown strength criterion and Goodman stiffness relation between intact and fractured rocks are employed. Ten rock types with strength varying from soft to strong rocks are used. A polyaxial load frame is used to load and unload the specimens, which allows determining the compressive strengths and deformation moduli of the rocks under both single and multi-stage testing.

2. SAMPLE PREPARATION

Rock specimens come from various locations in Thailand. Rock specimens are prepared from ten different rock types, ranging from soft to hard rocks, including Tak Fa gypsum, Maha Sarakham salt, Khao Khad bedded limestone, Phu Kradung sandstone, Khao Khad marble, Pha Wihan sandstone, Phu Phan bedded sandstone, Phu Phan sandstone, Rayoung-Bang Lamung granite, and Buriram basalt. Prismatic specimens are prepared with nominal dimensions of 54 × 54 × 108 mm³. The bedding planes for sedimentary rocks are oriented perpendicular to the primary axis

3. TEST METHOD

There are two types of triaxial tests: single stage triaxial compression tests and multi-stage triaxial compression tests. The objective of the triaxial compression tests is to determine the parameters (m and s) of the specimens in accordance with the Hoek-Brown criterion [7] under varying confining pressures. After the confining pressure is increased a desired magnitude, the axial stress increases at rate of 1 MPa/s until failure occurs while the confining pressure is maintained constant. To find the strength envelope, the specimens are tested at different confining pressures in a single-stage behavior under axial stress until it fails, as per the ASTM standard procedure (ASTM D7012-14) [1]. The multi-stage triaxial compression testing aims to measure the maximum failure stress and axial and lateral strains during loading and reloading phases by conducting a multi-stage loading using polyaxial compression frame [8]. These tests are carried out under constant confining pressures between 0 and 40

MPa. The multi-stage stress path is shown in **Fig 1.** Under hydrostatic conditions, confining pressure (σ_3) and axial (σ_1) stress are first simultaneously increased to the required confining pressure. The axial stress is then raised to failure and then released to the original confining pressure. Both axial and confining stresses then increased to the next level of confining pressure. After that, axial stress is once raised to reach the peak strength. This cycle is repeated to allow analysis of rock strength at various confining pressures. Axial stress and strains and lateral strains are plotted continuously from the first to the last loading stages.

4. TEST RESULTS

The results of single stage triaxial compression tests conducted under confining pressures (σ_3) ranging from 0 to 40 MPa. They are performed to compare with the multi-stage triaxial tests. Extension failure is observed in high-loading specimens. The high confining pressures result in multiple fractures. Some post-tested single stage specimens are shown in **Fig 2(a).** The results of multi-stage triaxial compression tests. These tests are performed to compare with the single stage triaxial tests. The specimens exhibit varying failure patterns depending on the applied stress level at each stage. Under confining pressure, deformation was observed to gradually increase as each subsequent step was initiated at a higher confining pressure.

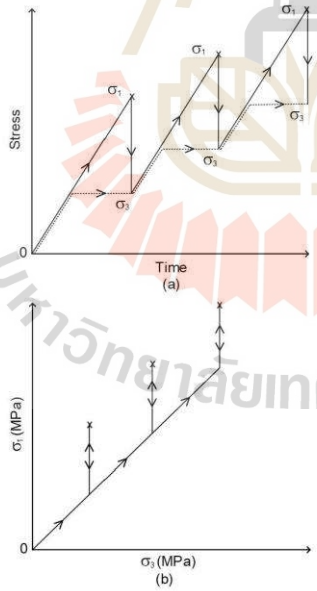

Fig.1. Stress path for multi-stage triaxial compression test used in this study, (a) variations over time and (b) confining pressure (σ_3).

Some post-tested multi-stage specimens are shown in **Fig 2(b).** The test results are presented as stress-strain curves in **Fig 3 and 4.**

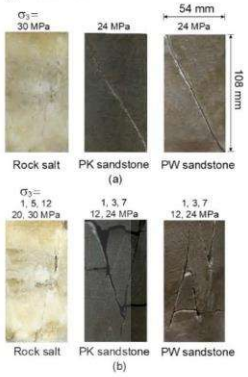

Fig.2. Some post-test specimens for single stage (a) and multi-stage triaxial compression tests (b).

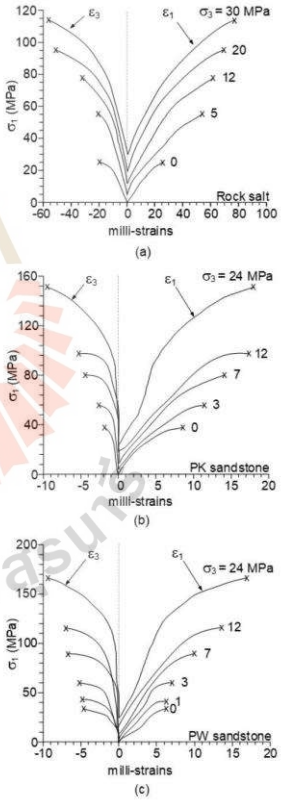

Fig.3. Some stress-strain curves obtained from Rock salt (a), PK sandstone (b), and PW sandstone (c) specimens with single stage triaxial compression tests.

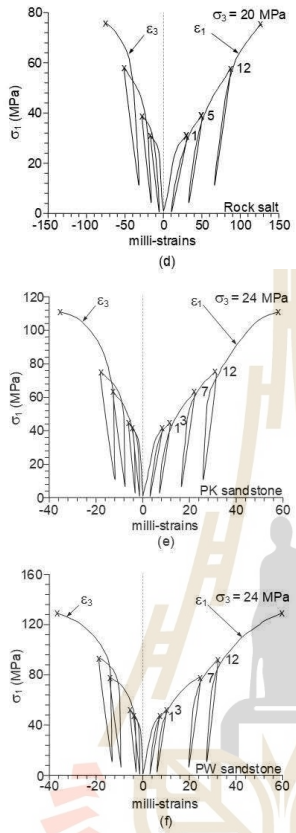

Fig.4. Some stress-strain curves obtained from Rock salt (d), PK sandstone (e), and PW sandstone (f) specimens with multi-stage triaxial compression tests.

4.1. Strength results

Hoek-Brown criterion [7] is applied to the triaxial compression strengths, using data obtained from both single and multi-stage test conditions, based on the compressive strengths of test results in **Table 1.** It represents the principal stresses at failure ($\sigma_{1,f}$):

$$\sigma_{1,f} = \sigma_3 + (\, m \cdot \sigma_e \cdot \sigma_3 + s \cdot \sigma_e^{\,2})^{1/2} \qquad (1)$$

where $\sigma_{1,f}$ is compressive strength at failure, σ_3 and σ_e are confining pressure and uniaxial compression strength of rock. The parameters m and s are empirical constants. Regression analyses are performed on the test results to determine these parameters. The $\sigma_{1,f} - \sigma_3$ curves obtained from the regression are compared with the test data for all rock types in **Fig 5.** Good correlations are obtained ($R^2 > 0.9$).

Table 1: Summary of single and multi-stage triaxial compression test results.

Rock Types	Confining pressure σ_3 (MPa)	$\sigma_{1,f}$ (MPa)	
		Single stage	Multi-stage
Tak Fa gypsum	0	10.8	-
	1	-	11.3
	3	17.9	13.3
	7	28.3	18.1
	12	40.8	24.6
	18	51.3	33.1
Maha Sarakham salt	0	25.1	-
	1	-	27.2
	5	55.3	35.9
	12	77.1	54.1
	20	95.6	71.5
	30	114.2	89.5
Khao Khad bedded limestone	0	32.6	-
	1	-	35.2
	5	64.2	50.3
	8	78.3	61.2
	16	107.1	85.6
	30	149.1	121.5
Phu Kradung sandstone	0	38.9	-
	1	-	40.4
	3	58.0	43.7
	7	77.7	62.4
	12	97.2	73.7
	24	151.3	110.7
Khao Khad marble	0	41.7	-
	1	-	43.5
	3	65.4	50.3
	7	83.2	66.3
	12	105.2	85.3
	20	139.7	109.3
	35	186.9	147.2
Pha Wihan sandstone	0	43.3	-
	1	-	46.8
	3	63.4	51.3
	7	88.9	76.6
	12	106.9	91.3
	24	166.4	129.0
Phu Phan bedded sandstone	0	53.7	-
	1	-	55.3
	3	78.3	63.5
	7	105.4	84.6
	12	130.2	108.4
	24	186.5	144.9
Phu Phansandstone	0	55.0	-
	1	-	57.2
	4	95.7	75.3
	12	138.8	110.5
	20	180.4	147.3
	36	235.9	195.3
Rayong-Bang Lamung granite	0	59.1	-
	1	-	61.0
	5	-	86.2
	10	140.3	115.4
	20	191.3	157.4
	30	225.3	191.9
Buriram basalt	0	100.6	-
	1	-	107.3
	10	192.1	175.3
	20	271.2	240.5
	30	331.9	290.3
	40	376.5	325.4

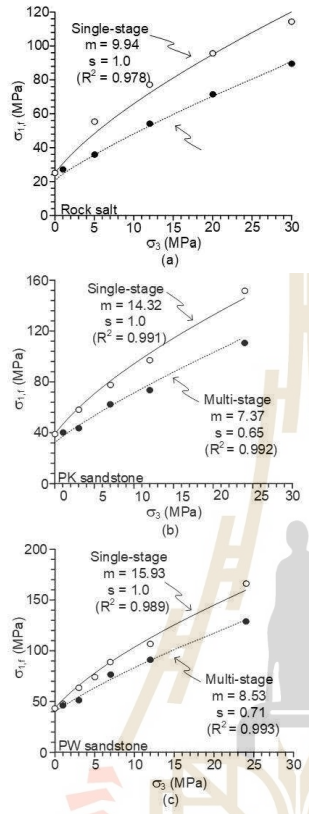

Fig.5. Compressive strengths at failure as a function of confining pressure for Maha Sarakham salt (a), Phu Kradung sandstone (b), Pha Wihan sandstone (c).

An attempt is made to correlate Hoek-Brown parameters obtained from the two test conditions. Since both parameters depend on uniaxial compression strength of rocks. They are plotted as a function of σ_c in **Fig 6.** The parameter m increases with σ_c. where single stage test condition gives higher values than the multi-stage condition. The parameter s for the single stage test is equal to one for all rock types as it is calibrated from the intact rocks. For multi-stage testing however parameter s shows the values of less than one. The weaker rocks give the lower s values than the stronger rocks (higher σ_c).

To correlate the Hoek-Brown parameters between the two test conditions, the subscript m denoting multi-stage is assigned for the multi-stage parameters (m_m and s_m), where subscript s (denoting single stage) is using for the single stage parameters (m_s and s_s). After several trials, ratios of the Hoek-Brown parameters are proposed as: m_m/m_s and s_m/s_s. They are plotted in **Fig 7**. Exponential equations are fitted to these ratios. Good correlation is obtained. They can be presented as:

$$m_m/m_s = 1 - a \cdot \exp(-b \cdot \sigma_c) \quad (2)$$

$$s_m/s_s = 1 - c \cdot \exp(-d \cdot \sigma_c) \quad (3)$$

when a, b, c, d are empirical constants. The m_m/m_s ratio allows predicting then m_s value for single stage testing of the m_m value is known for the multi-stage testing. Extrapolation of the two equations above allows predicting the uniaxial compressive strengths of rocks at which the m_m/m_s and s_m/s_s approach one are given in **Table 2.**

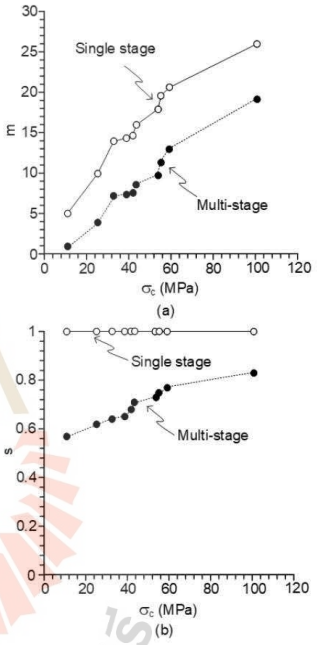

Fig.6. Hoek-Brown parameters, m (a), and s (b) as a function of uniaxial compressive strength (σ_c).

4.2. Strengths from researches obtained elsewhere

Fig 8 compares the m_m/m_s ratio obtained from this study with those published by other researches who conduct both multi-stage and single stage compression testing on various rock types. The solid points in the diagram represent the results obtained from the same loading path are used in this study. The open data points are those from different loading paths of multi-stage testing. The error between the prediction and the results obtained elsewhere are calculated using equations as follows [9]:

$$\text{Error} = 1/n \left| m_m/m_{s\,(i,p)} - m_m/m_{s\,(i,t)} / m_m/m_{s\,(i,p)} \right| \cdot 100 \quad (4)$$

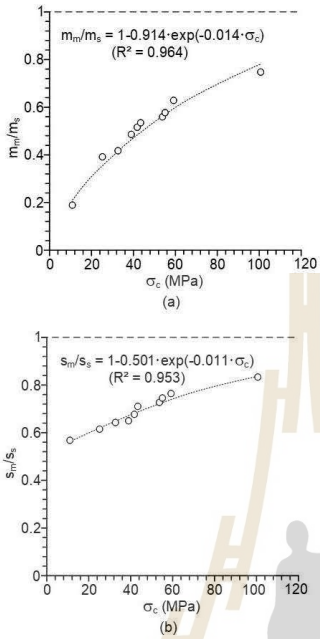

Fig.7. Relationship between m_m/m_s ratios (a), and s_s/s_m ratios (b) as a function of uniaxial compressive strength (σ_c).

Table 2: m_m/m_s and s_m/s_s ratios obtained from single and multi-stage strength results.

Rock Types	m_m/m_s	s_m/s_s
Tak Fa gypsum	0.19	0.57
Maha Sarakham salt	0.39	0.62
Khao Khad bedded limestone	0.42	0.64
Phu Kradung sandstone	0.43	0.65
Khao Khad marble	0.51	0.68
Pha Wihan sandstone	0.54	0.71
Phu Phan bedded sandstone	0.56	0.73
Phu Phan sandstone	0.58	0.75
Rayong-Bang Lamung granite	0.63	0.77
Buriram basalt	0.74	0.83

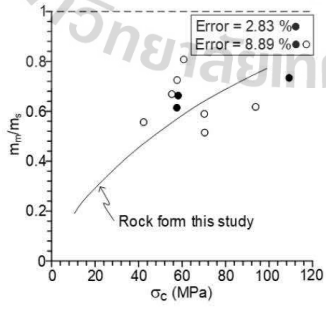

Fig.8. Solid points are results from [3]. Open points are from others: [9], [10], [11], [12].

DISCUSSIONS

Due to the fact that the $\sigma_{1,f} - \sigma_3$ relations for all tested rocks are not linear, as shown in **Fig 5,** the conventional Coulomb strength criterion is not applicable here. In addition, the criterion is only for intact rock specimens, and hence it is not valid for the multi-stage testing specimens where they are failed after the first loading cycle. Hoek-Brown criterion seems more appropriate for this study as it is capable of describing the compressive strengths of the intact specimens for the single stage tests and the failed specimens for multi-stage testing.

Rock types selected for this study have uniaxial compressive strengths ranging from soft rock (gypsum – 10.8 MPa) to strong rock (basalt – 100.6 MPa). This allows deriving an appropriate mathematical relations between m_m/m_s ratios and the strength (i.e., Equation (2)). Missing from this study is the very strong rock specimens (σ_c > 250 MPa), as they are rarely encountered in the geo-engineering projects and mines in Thailand.

Good correlations between m_m/m_s ratio and σ_c and between s_m/s_s ratio and σ_c support that the triaxial compression strengths for the single stage testing that uses several specimens to accomplish can be predicted by the results of the multi-stage testing that uses much fewer specimens. As a minimum the multi-stage testing requires only one uniaxial compression test to obtain σ_c and one multi-stage triaxial testing to obtain m_m and s_m. The three parameters can be used to predict m_s and s_s (always equals to 1) for the single stage testing.

Comparison of the correlation equation obtained from this study with the multi-stage strength results obtained elsewhere by other researchers suggests that the multi-stage strengths are sensitive to the loading path. If a multi-stage testing uses the same loading path that used here the prediction by Equation (2) can give good correlation with the error of about 2.83%, as shown in **Fig 8.** For multi-stage strengths obtained under different loading paths (i.e., not allowing axial stress to drop from the failure stress to the current confining pressure), as performed by [10], [11], and [12], larger error can be obtained, as shown in **Fig 8.**

CONCLUSIONS

Test results and analyses performed in this study can be concluded as follows.

1. Hoek-Brown criterion can be used to correlate the triaxial compressive strengths between single and multi-stage testing.
2. Good correlation between m_m/m_s ratio and uniaxial compressive strength allows predicting the conventional single stage triaxial compressive strengths from the multi-stage compressive strength results.

3. The multi-stage triaxial strengths are sensitive to the loading paths used for each loading cycle. Different sets of compressive strengths would likely be obtained under different loading paths.

ACKNOWLEDGMENTS

This study is funded by Suranaree University of Technology and by the Higher Education Promotion and National Research University of Thailand. Permission to publish this paper is gratefully acknowledged.

REFERENCES

[1] ASTM D7012-14e1, Standard Test Methods for Compressive Strength and Elastic Moduli of Intact Rock Core Specimens under Varying States of Stress and Temperatures, ASTM International, West Conshohocken, PA, 2014.

[2] G. Wang, X. Feng, T. Yang, C. Yang, Q. Han, and R. Kong, "Experimental study of the mechanical characteristics of jinping marble under multi-stage true triaxial compression testing," *Rock Mechanics and Rock Engineering*, vol. 55, no. 2, pp. 953–966, 2022.

[3] S.-Q. Yang, "Strength and deformation behavior of red sandstone under multi-stage triaxial compression," *Canadian Geotechnical Journal*," vol. 49, no. 6, pp. 694–709, 2012.

[4] K. Kovári, and A. Tisa, "Multiple failure state and strain controlled triaxial tests," *Rock mechanics*, Springer-Verlag, vol. 7, pp. 17–33, 1975.

[5] S. Melati, R.K. Wattimena, S. Kramadibrata, G.M. Simangunsong, and R.G. Sianturi, "Stress paths effects on multistage triaxial test," *ISRM International Symposium-Asian Rock Mechanics Symposium*, pp. ISRM–ARMS8, 2014.

[6] E. Hoek, and E.T. Brown, "Underground excavation in rock," *Institution of Mining and Metallurgy*, London, 1980.

[7] J.C. Jaeger, N.G.W. Cook, and R.W. Zimmerman, "Fundamentals of rock mechanics," 4th ed. Oxford: Blackweel, 2007.

[8] U. Khair, H. Fahmi, S. Al Hakim, and R. Rahim, "Forecasting error calculation with mean absolute deviation and mean absolute percentage error," *Journal of physics: Conference series*, vol. 930, no. 1, 2017.

[9] M. Aghababaei, M. Behnia, and O. Moradian, "Experimental investigation on strength and failure behavior of carbonate rocks under multistage triaxial compression," *International Journal of Rock Mechanics and Mining Sciences*, pp. 1365–1609, vol. 123, 2019.

[10] X. Shia, L. Liua, Y. Menga, S. Maoa, W. Wanga, J. Wua, and C. Wena, "Correction model for strength parameters of a multistage triaxial compression test on sandstone," *In Proceedings of the First Southern Hemisphere International Rock Mechanics Symposium*, pp. ISRM–ARMS9, 2016.

[11] J. Venter, C. Purvis, and J. Hamman, "Hoek–Brown mi estimation–a comparison of multistage triaxial with single stage triaxial testing," *In APSSIM 2016: Proceedings of the First Asia Pacific Slope Stability in Mining Conference*, Australian Centre for Geomechanics. pp. 289–299, September 2016.

[12] P. Cain, C. M. Yuen, G. R. Le Bel, A. M. Crawford, and D. H. Lau, "Triaxial testing of brittle sandstone using a multiple failure state method," Geotechnical Testing Journal, vol. 10, no. 4, pp. 213–217, 1987.

★★★

BIOGRAPHY

Mr. Thanawat Sasen was born on August 29, 2000 in Samutprakarn, Thailand. He received his Bachelor's Degree in Engineering (Geological Engineering) from Suranaree University of Technology in 2021. After graduation, he continued to study with a Master's degree in the Geological Engineering Program, Institute of Engineering, Suranaree university of Technology. During graduation, 2021-2023, he was a part time worker in position of research associate at the Geomechanics Research Unit, Institute of Engineering, Suranaree University of Technology.